



THE HONG KONG
POLYTECHNIC UNIVERSITY

香港理工大學

Pao Yue-kong Library
包玉剛圖書館

Copyright Undertaking

This thesis is protected by copyright, with all rights reserved.

By reading and using the thesis, the reader understands and agrees to the following terms:

1. The reader will abide by the rules and legal ordinances governing copyright regarding the use of the thesis.
2. The reader will use the thesis for the purpose of research or private study only and not for distribution or further reproduction or any other purpose.
3. The reader agrees to indemnify and hold the University harmless from and against any loss, damage, cost, liability or expenses arising from copyright infringement or unauthorized usage.

If you have reasons to believe that any materials in this thesis are deemed not suitable to be distributed in this form, or a copyright owner having difficulty with the material being included in our database, please contact lbsys@polyu.edu.hk providing details. The Library will look into your claim and consider taking remedial action upon receipt of the written requests.



THE HONG KONG POLYTECHNIC UNIVERSITY

**DEPARTMENT OF
APPLIED BIOLOGY & CHEMICAL TECHNOLOGY**

*The Study of Macroporous Adsorption Resin (MAR) on
Preparative Separation and Purification of Saikosaponins from
the Crude Herbal Extract*

Cheung Bo Lin

**A thesis submitted
in partial fulfillment of the requirements**

for

The Degree of Master of Philosophy

8-2006



**Pao Yue-kong Library
PolyU • Hong Kong**

Certificate of originality

I hereby declare that this thesis is my own work and that, to the best of my knowledge and belief, it reproduces no material previously published or written, nor material that has been accepted for the award of any other degree or diploma, except where due acknowledgement has been made in the text.

_____ (Signed)

CHEUNG BO LIN (Name of student)

Abstract

Study was carried out to investigate the adsorption characteristics of saikosaponins a, c and d on the macroporous adsorption resins and the efficiency of the adsorption column for the separation and purification of saikosaponins from the crude herbal extract. Both static and dynamic experiments were conducted.

In static studies, the performances of eight macroporous resins namely HPD100, HPD300, HPD400, HPD450, HPD500, HPD600, HPD700 and HPD800 for the adsorption of saikosaponins were evaluated. HPD100 was found to have the highest adsorption capacity. It indicated that the hydrophobic property of the resin played a significant role in the adsorption. The effects of temperature, initial saikosaponins concentration and pH on the adsorption on HPD100 were also investigated. The results showed that higher temperature and initial saikosaponins concentration could enhance the adsorption while the effect of pH was not significant. Furthermore, HPD100, HPD450 and HPD600 were selected for the studies of isotherms, kinetics and thermodynamic of adsorption. The adsorption data from the HPD100 resin fit well to the Langmuir model indicating the adsorption was monolayer, while those from the HPD450 and HPD600 resins fit to either the Langmuir model or the Freundlich model indicating the adsorption was either monolayer or multilayer. The

positive value of the adsorption enthalpy and the negative value of the Gibbs free energy showed that the adsorption process was endothermic and spontaneous in nature, respectively. The adsorption on HPD100, HPD450 and HPD600 resins followed either the pseudo first order kinetic or the pseudo second order kinetic. The rate of adsorption process was found to be controlled by the film diffusion.

In dynamic studies, the adsorption and desorption experiments were carried out on a column packed with HPD100 resin. The operating parameters including feed flow rate, feed concentration and bed depth were varied to investigate their effects on the adsorption performance of the column. The results show the breakthrough occurred earlier when the feed flow rate and feed concentration increased. In contrast, the breakthrough took place later when the bed depth increased. An efficient column operation of the adsorption step was obtained.

In the elution step, step-gradient elution program with 120 ml 0%, 160 ml 25%, 160 ml 45%, 160 ml 65% and 120 ml 85% aqueous ethanol in succession was found to be the most proper program to achieve an efficient separation. The purity, concentration ratio and recovery yield of saikosaponins were ~ 20%, ~17 and ~70% respectively. In order to determine the reusability of the column, the adsorption/desorption (A/D)

cycle was repeated a number of times. The results showed that after five successive A/D cycles, the column was able to retain over 50% adsorption capacity.

Acknowledgements

I would like to express my thankfulness to Dr. H.H. Liang who not only provided an opportunity for me to do this research, but also give me valuable guidance and comments on this research. In addition, I am also grateful to thank Dr. Liang's research group members, including Mr. Hu Zhuo Yan and Miss Zhao Shuna for their advice and their helps in seeking the technical support of research facilities and the samples of Radix Bupleuri.

Table of contents

	Page
1. Introduction	1-4
2. Literature review	
2.1 The herb	
2.1.1 General information	5-8
2.1.2 Intake methods	9
2.2 Techniques for separating and purifying active ingredients from Chinese herbs	10-12
2.3 Macroporous adsorption resin (MAR)	
2.3.1 General information	12-14
2.3.2 Adsorption mechanism	15-19
2.3.3 Commercially available resins	20-23
2.4 Isolation and purification of active ingredients of TCMs by MAR	23-24
2.4.1 Static experiments	
2.4.1.1 Selection of the resin	24-25
2.4.1.2 Determination of adsorption isotherms	26
2.4.1.3 Determination of adsorption kinetic	27
2.4.2 Dynamic experiments	27-28
2.4.3 Factors affecting the adsorption of active ingredients in TCMs	28-29
2.5 Application of MAR in previous research	
2.5.1 Natural products	29-30
2.5.2 Saponins in TCMs	30-32
3. Materials and methods	
3.1 Reagents	33

3.2 Adsorbents	33-34
3.3 Preparation of crude Chai Hu extracts	35
3.4 HPLC analysis of saikosaponins a, c and d	35-36
4. Static study	
4.1 Experimental section	
4.1.1 Static adsorption	37-38
4.1.2 Static desorption	38-39
4.1.3 Adsorption isotherms	39
4.1.4 Adsorption kinetic	40
4.2 Results and discussion	
4.2.1 Selection of adsorption resins	41-47
4.2.2 Characterization of the polymer adsorbents	47-48
4.2.3 Effect of temperature	49
4.2.4 Effect of initial saikosaponins concentration	49-51
4.2.5 Effect of pH	52-53
4.2.6 Adsorption isotherms	54-64
4.2.7 Thermodynamic of adsorption	64-68
4.2.8 Adsorption kinetics	68-76
5. Dynamic study	
5.1 Experimental section	
5.1.1 Adsorption separation process	77
5.1.2 Low pressure liquid chromatography (LPLC) system and column conditioning	77-78
5.1.3 Dynamic adsorption	78-79
5.1.4 Dynamic desorption	79

5.1.5 Evaluation of the column performance	80-81
5.2 Results and discussion	
5.2.1 Dynamic adsorption	
5.2.1.1 Effect of feed flow rate	82-84
5.2.1.2 Effect of feed concentration	85-86
5.2.1.3 Effect of bed depth	87-88
5.2.1.4 Concentration profiles of saikosaponins in the fixed-bed	89-90
5.2.1.5 Breakthrough curve	90-91
5.2.2 Dynamic desorption	
5.2.2.1 Elution solvent	92-94
5.2.2.2 Dynamic elution curve	94-97
5.2.2.3 Comparison of the column performance	98-109
5.2.2.4 Reusability of the column	109-111
6. Conclusions	112-114
7. Recommendations	115-116
8. Appendices	117-119
References	120-124

List of figures

- Figure 2.1 The chemical structures of saikosaponin a, saikosaponin c and saikosaponin d.
- Figure 2.2 The formation of induced dipole.
- Figure 2.3 The lone pair electrons on ammonia, water and hydrogen fluoride molecules.
- Figure 2.4 The hydrogen bonding between two water molecules.
- Figure 3.1 HPLC chromatogram at wavelength 210 nm of ssa, ssc and ssd standards.
- Figure 3.2 Calibration curve for saikosaponins standards.
- Figure 4.1 The plot of pore size distribution along pore diameter for HPD100, HPD450 and HPD600 resins.
- Figure 4.2 The pore system (cited from Klaus et al.,1995)
- Figure 4.3 Effects of initial saikosaponins concentration and temperature on the adsorption capacity of HPD100 resin at conditions: adsorbent dosage 1.00 ± 0.01 g, pH 5.0 ± 0.1 , agitation 150 rpm.
- Figure 4.4 Effect of pH on saikosaponins adsorption on HPD100 at conditions: adsorbent dosage 1.00 ± 0.01 g, agitation 150 rpm.
- Figure 4.5 The adsorption isotherms of saikosaponins on HPD100 resin at different temperatures.
- Figure 4.6 The adsorption isotherms of saikosaponins on HPD450 resin at different temperatures.
- Figure 4.7 The adsorption isotherms of saikosaponins on HPD600 resin at different temperatures.
- Figure 4.8 The adsorbent structure (cited from Klaus et al., 1995)
- Figure 4.9 Langmuir isotherm for HPD100 (the plot of $1/Q_e$ against $1/C_e$).

Figure 4.10 Langmuir isotherm for HPD450.

Figure 4.11 Langmuir isotherm for HPD600.

Figure 4.12 Freundlich isotherms for HPD100 (the plot of $\ln Q_e$ against $\ln C_e$).

Figure 4.13 Freundlich isotherm for HPD450.

Figure 4.14 Freundlich isotherm for HPD600.

Figure 4.15 The Van't Hoff plot

Figure 4.16 The adsorption capacities of saikosaponins on HPD100, HPD450 and HPD600 resins as a function of time (pH 5.0 ± 0.1 , 1.00 ± 0.01 g adsorbent, temperature 298.0 ± 0.5 K and agitation 150 rpm).

Figure 4.17 The plots of the pseudo-first order kinetics on the three resins.

Figure 4.18 The plots of pseudo second-order kinetics on the three resins.

Figure 4.19 The diffusion of adsorbate (cited from Klaus et al.,1995)

Figure 5.1 The breakthrough curves of saikosaponins adsorption in various three feed flow rates. ($T = 25.0 \pm 0.5^\circ\text{C}$, $C_{in} = 0.188 \pm 0.007$ mg/ml and $BD = 12\text{cm}$)

Figure 5.2 The breakthrough curves of saikosaponins adsorption in various feed concentrations. ($T = 25.0 \pm 0.5^\circ\text{C}$, feed flow rate = 2 ml/min and $BD = 12\text{cm}$)

Figure 5.3 The breakthrough curves of saikosaponins adsorption in various bed depths. ($T = 25.0 \pm 0.5^\circ\text{C}$, feed flow rate = 2 ml/min and $C_{in} = 0.317 \pm 0.011$ mg/ml)

Figure 5.4 The concentration profiles for adsorption in a fixed bed. (cited from Warren et al.,2005)

Figure 5.5 The Breakthrough curve for adsorption in the fixed bed.

Figure 5.6 The dynamic elution curves for step-gradient elution program (1): (a) purity of saikosaponins, (b) mass of saikosaponins and (c) Total mass of effluent.

Figure 5.7 The dynamic elution curves for the step-gradient elution program (2): (a) purity of saikosaponins, (b) mass of saikosaponins and (c) Total mass of effluent.

Figure 5.8 The dynamic elution curves for the step-gradient elution program (3): (a) purity of saikosaponins, (b) mass of saikosaponins and (c) Total mass of effluent.

Figure 5.9 The dynamic elution curves for the step-gradient elution program (4): (a) purity of saikosaponins, (b) mass of saikosaponins and (c) Total mass of effluent

List of tables

Table 3.1 Physical properties of HPD series resins

Table 4.1 The adsorption capacities and adsorption efficiencies of individual saikosaponin on the eight resins

Table 4.2 The adsorption capacities, adsorption efficiencies and desorption efficiency of total saikosaponins on the eight resins

Table 4.3 Langmuir parameters

Table 4.4 Freundlich parameters

Table 4.5 Thermodynamic parameters for the adsorption process of saikosaponins on three resins

Table 4.6 The parameters of adsorption kinetics for saikosaponins on the three resins

Table 4.7 The diffusion rate parameters

Table 5.1 The experimental conditions for column tests

Table 5.2 The BV, BT and A A at the breakthrough points in three feed flow rates

Table 5.3 The BV, BT and A A at the breakthrough points in three feed concentrations

Table 5.4 The BV, BT and A A at the breakthrough points in three bed depths

Table 5.5 Four step-gradient elution programs

Table 5.6 Column performances of the step-gradient elution program (1)

Table 5.7 Column performances of the step-gradient elution program (2)

Table 5.8 Column performances of the step-gradient elution program (3)

Table 5.9 Column performances for the step-gradient elution program (4)

Table 5.10 The column performance indices for the 4 step-gradient elution programs

Table 5.11 The effects of A/D cycles on separation performance of column for saikosaponins

1. Introduction

It is a long history of the Chinese people using Traditional Chinese Medicines (TCMs) and herbs to prevent and treat various illnesses. Based on thousands of years of experience, the therapeutic values of most TCMs have been discovered. There are 992 monographs of Chinese crude drugs and Chinese traditional patent medicines recorded in the Chinese pharmacopoeia. (The State Pharmacopoeia Commission of PRC, 2000). The TCMs are also widely used all over the world in some Asian countries such as Japan, Korea and India, and even in some European and North American countries (Li et al., 1998).

The most common and conventional processing method of TCMs is decoctions. Decoction is the process by which TCMs are boiled and the remaining liquid is used for treatment purposes. However, decoctions have several drawbacks. Preparing decoctions is a time-consuming process in today's fast-paced society. In addition, the patients have to take in large volume of crude herbal extract. Furthermore, the herbal extract is a complex mixture containing different components such as proteins, sugars, mucilage and tannin in addition to the desired active components of the TCMs. Thus, the patients have to take in large amounts of side products.

During the modernization of TCMs, more convenient herbal dosage forms have been developed by modern pharmaceutical technology. The active components are separated and purified from the bulk of herbal extract and made into various dosage forms such as tablets, capsules, soluble granules, intravenous and intramuscular injections. It not only solves problems such as inconvenience of preparation and administration of decoctions but also improves the quality of the herbal products.

Organic solvent extraction and adsorption are two of the conventional techniques for separating and purifying active components from crude TCMs (Shanghai Institute of Materia Medica, Chinese Academy of Sciences, 1983). By considering the economic and environmental aspects, the first technique is used less and less these days as lots of organic solvent are exhausted and discharged. The traditional adsorbents used in adsorption include silica gels, alumina and activated carbons. Because of their weak mechanical intensity and uneasy regeneration, they have been substituted by newly developed macroporous polymeric adsorbents in recent years.

Macroporous adsorption resin is one of newly developed techniques to separate and purify active components from the herbal extract. It is of a non-ionic porous polymer with a significantly large surface area. The network property, pore structure and

functional groups of the resins can be tailor made to certain degree for selectively adsorbing specific groups of organic molecules. Its high loading capacity made it possible to perform on a large scale. It has been widely applied in wastewater treatment, pharmaceutical and food industries. In the past decade, it has been successfully applied in the separation and purification of active components from the TCMs. A number of published literatures showed that it is mainly applied in isolating saponins, flavonoids and alkaloids in the medicinal herbs (Mi et al., 2001; Tu et al., 2004; Li and Li, 2005).

The main aim of this study was to develop a guideline for the selection of adsorption resins for the preparative separation of active components from Chai Hu extract or other herbal materials in general, as well as the design and operation of adsorption column for separating and purifying active components of the Chinese medicinal herbs. Besides, the efficiency and economy of the adsorption column for separation and purification were investigated.

The adsorption characteristics of the active components of a Chinese medicinal herb, Chai Hu (*Radix Bupleuri*), on different macroporous adsorption resins were evaluated. Its active components are saikosaponins a, c and d which exhibit anti-inflammatory,

sedative and antipyretic activities (Heidelbert et al., 1996). Both static and dynamic experiments were carried out.

In static experiments, the effects of the resin structures and different experimental parameters such as temperature, initial saikosaponins concentration and pH of sample solution on adsorption were investigated. In addition, adsorption isotherms, kinetics and thermodynamic were also explored.

In dynamic experiments, the effects of operating parameters such as feed flow rate, feed concentration and bed depth on the adsorption performance of the column were determined. Besides, a proper step-gradient elution program was developed to achieve an efficient separation.

2. Literature review

2.1 The herb

2.1.1 General information

In Chinese pharmacopoeia, Chai Hu is the dried root of *Bupleurum chinense* DC. (Bei Chai Hu) or *Bupleurum scorzonerifolium* Willd. (Nan Chai Hu). Bei Chai Hu and Nan Chai Hu are different species. They differ both in their morphology and in their origin. These herbs are members of the Apiaceae (Umbelliferae) family. In Japanese pharmacopoeia, Chai Hu is the dried root of *Bupleurum falcatum* L. or varieties of this species. Its Japanese name is saiko. Its Korean name is siho (Heidelbert et al., 1996; WHO, 1999; Chen et al., 2004).

The original source is Shen Nong Ben Cao Jing. Bei Chai Hu originates from the northern part of China (north of the Yellow River) such as Hebei, Henan, Hubei, Shanxi and Liaoning. It is generally used as the standard source for Chai Hu. Nan Chai Hu originates from the southern part of China such as Sichuan and Anhui. Besides China, Cha Hu is distributed in northern Asia and Europe (Heidelbert et al., 1996; WHO, 1999; Chen et al., 2004).

Bei Chai Hu is cylindrical or elongated conical in shape, 6-15 cm long and 0.3 – 0.8 cm in diameter. It is frequently branched at the lower part. Externally, it is blackish-brown or light brown. The texture is hard and tenacious so it is not easy to break. The odour is slightly aromatic and the taste is slightly bitter. Nan Chai Hu is relatively thin and conical root. It is usually non or slightly branched at the lower part. Externally, it is reddish brown or blackish-brown. The texture is slightly soft so it is easy to break. The odour is rancid (Heidelbert et al., 1996). The dried Chai Hu is shown in Picture 2.1.

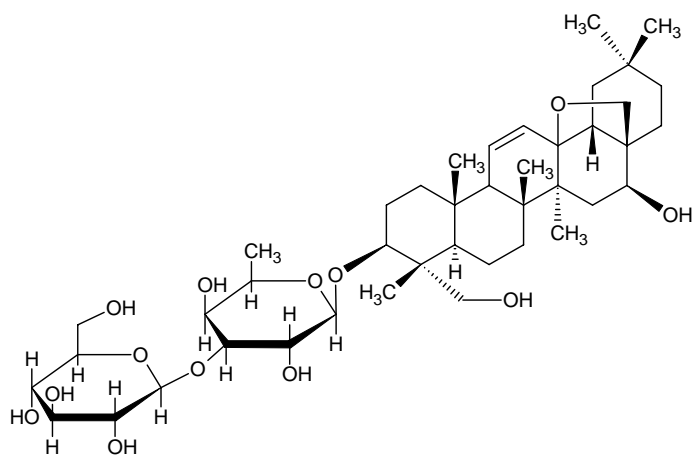


Picture 2.1 Dried Chai Hu.

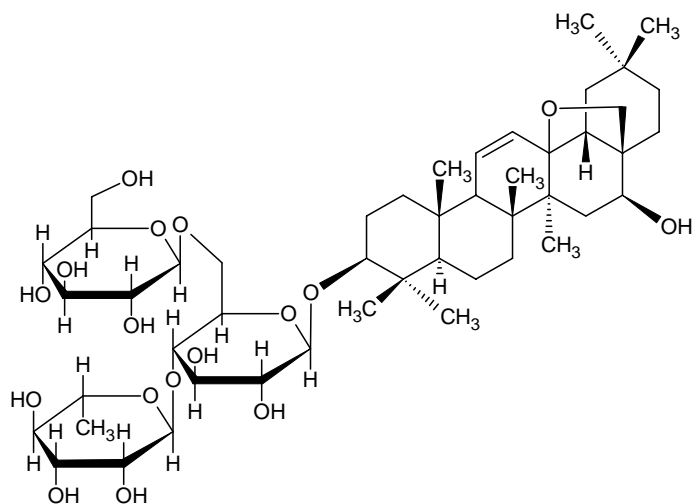
Chai Hu is propagated from seed in spring or by root division in autumn. Its growth requires well-drained soil and plenty of sunlight. The root is dug up in spring or autumn. The stems, leaves and soil are removed from the root which is then dried in the sun and cut into short pieces. The dried roots are stored in a ventilated dry place and protected from moth, light and moisture (The State Pharmacopoeia Commission of P.R. China, 2000).

Chai Hu is pungent and bitter in flavour, slightly “cold” in nature. It harmonizes the exterior and the interior, spreads the liver and relieves liver qi stagnation, and lifts yang qi with its ascending and dispersing functions (Heidelbert et al., 1996; WHO, 1999). Chai Hu is an important herb to treat shaoyang syndrome. The symptoms of the syndrome include alternate spells of chills, common cold with fever, distending pain in the chest and hypochondriac regions. It is also used to treat other symptoms including inflammation associated with influenza, menstrual disorders, hemorrhoids, prolapse of the uterus and rectum (Heidelbert et al., 1996).

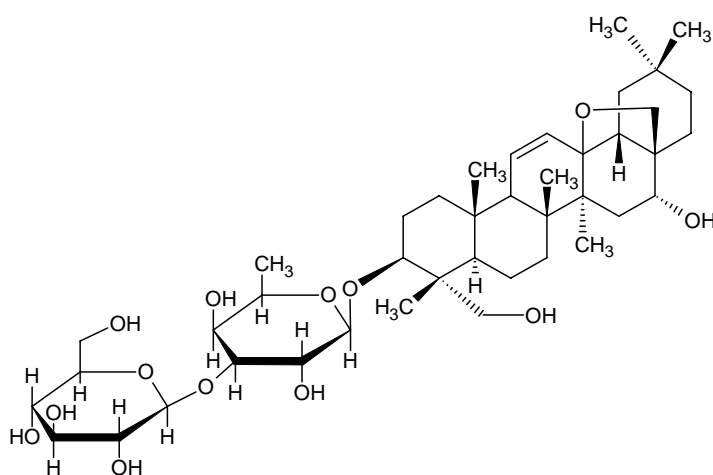
Saikosaponins are the major active ingredients of Chai Hu. In particular, saikosaponins a, c and d are three of the major saponins in this group ingredient. Their chemical structures are shown in Fig.2.1. They have demonstrated several pharmacological effects including antipyretic and analgesic activity, sedative effects, anti-inflammatory activity, immune regulation activity, anti-hyperlipidemic activity and anti-proliferative activity. The HPLC chromatogram of the saikosaponins a, c and d in the crude Chai Hu extract is shown in Appendix A.1. In addition to the saikosaponins, polysaccharides are the second major active ingredients of Chai Hu. They have exhibited some pharmacological effects including anti-ulcer activity and immune regulation activity (Heidelbert et al., 1996; WHO, 1999).



Saikosaponin a



Saikosaponin c



Saikosaponin d

Figure 2.1 The chemical structures of saikosaponin a, saikosaponin c and saikosaponin d.

2.1.2 Intake methods

Xiao Chai Hu Tang (Minor Bupleurum decoction) is a traditional Chinese formula prepared by traditional preparation procedure. Xiao Chai Hu Tang consists of Bupleuri (Chai Hu), Radix Scutellariae Baicalensis (Huang Qin), Rhizoma Pinelliae Ternatae (Ban Xia), Radix Panacis Ginseng (Ren Shen), uncooked Rhizoma Zingiberis Off icinalis (Sheng Jiang), Fructus Zizyphi Jujubae (Da Zao) and Radix Glycyrrhizae Uralensis (Gan Cao). The decoction was boiled in water and administrated per day. One course of treatment requires 4 weeks administration. Traditionally, Chinese people take it to treat alternating fever and chills, dry throat, bitter or sour taste in mouth, dizziness, irritability, chest and hypochondriac fullness, heartburn, nausea and vomiting.

Nowadays, more convenient dosage forms with small dosage sizes are developed by combining modern technological processing of traditional Chinese herbs and western medicine principles. These forms include tablets, capsules, soluble granules, suppositories and intravenous and intramuscular injections. These forms are more user friendly as they are easier to carry and swallow.

2.2 Techniques for separating and purifying active ingredients from Chinese herbs

With the modernization of Traditional Chinese Medicines (TCMs), the active ingredients of the herbs are separated and purified from the bulk of the herbal extract and then made into various convenient dosage forms.

Organic solvent extraction and activated carbon adsorption are two of the conventional techniques for separating and purifying active ingredients from crude herbs (Shanghai Institute of Materia Medica, Chinese Academy of Science, 1983).

However, these two techniques have several drawbacks. A large amount of organic solvent is exhausted in organic solvent extraction. While in activated carbon adsorption, the activated carbon is costly to regenerate, thus it can be used only once and generates a considerable amount of solid waste. It also tends to adsorb most organic chemicals indiscriminately, making it difficult to selectively recover certain organic chemicals for reuse. Macroporous adsorption resin (MAR) technology, a modern technique to separate and purify active ingredients from crude herbs, can overcome these problems. This technique can reduce the cost of operation because of its less consumption of extraction solvents and reusable adsorbents. Besides, the network property, pore structure and functional groups of resins can be tailor made to

certain degrees for selectively adsorbing specific groups of organic chemicals. Moreover, the resins are easily regenerated and the adsorbed active ingredients of TCMs are recovered for use by organic solvents elution. Furthermore, their high loading capacity made it possible to separate compounds in large amounts. Therefore, this technique can be performed on a large scale (Dong, 2001).

Nowadays, the common large scale separation and purification techniques are preparative thin liquid chromatography (PTLC), low pressure liquid chromatography (LPLC) and preparative high performance liquid chromatography (HPLC). The purity of purified ingredients obtained by PTLC and LPLC is not certain and the separated fractions often need to be further purified by preparative HPLC. Components purified by preparative HPLC are always in high purity. However, the operation cost of preparative HPLC is quite high as lots of solvents are exhausted as mobile phase in each run (Li et al., 1998).

Therefore, it is necessary to develop new techniques which are efficient, inexpensive and easy to scale-up into industrialized usage. In recent years, MAR has been developed as a new technique performed on a large scale for separating and purifying active ingredients of TCMs. This technique is still under development and further

study is necessary to investigate its efficiency and economy.

2.3 Macroporous adsorption resin (MAR)

Macroporous adsorption resins were first developed in the 1960s. These materials are porous polymeric spherical beads with a variety of surface polarities, surface areas and pore-size distributions. They are capable of effectively adsorbing organic molecules from aqueous solutions due to their highly porous polymeric structures with internal surfaces. The organic molecules are desorbed from the resin by solvent elution and may be recovered for use. The resin can be tailor made to selectively adsorb certain groups of organic molecules by varying surface polarity and pores structures such as surface areas and average pore-size distributions during manufacturing processes (Mi et al., 2001; Tu et al., 2004).

2.3.1 General information

The synthesis of macroporous adsorption resins is based on manufacturing technology of ion-exchange resins. They are synthesized by suspension copolymerization of a monomer e.g. styrene, acrylate and a cross linking agent e.g. divinylbenzene. Polymerization takes place in the presence of a pore-forming agent which is soluble in monomer mixture but itself is a poor solvent to the copolymer. The pore-forming

agent is removed from the polymeric network after polymerization and a porous structure with mechanical stability is left. The resin structure is modified by varying polymerization conditions such as the amounts of monomers and pore-forming agents used in the polymerization reaction (Xu et al., 2002).

Such made macroporous resins are white, milky white or pale yellow spherical beads with 20-60 mesh in sizes. They are polymeric adsorbents with excellent physical, chemical and thermal stability. They can work under 150°C. They are also stable at all pH range in aqueous solution. Their water content is around 40% to 70% (Wang et al., 2001; Tu et al., 2004).

The resins are mainly divided into three types – non-polar resins, medium polar resins and polar resins. For non-polar resins, they usually exhibit non-polar or hydrophobic behavior and so adsorb non-polar organic molecules from polar solvents such as water. For polar resins, they usually exhibit polar or hydrophilic behavior and adsorb organic molecules with some degree of polarity from non-polar solvents such as hydrocarbons. For medium polar resins, they exhibit both hydrophobic and hydrophilic behaviors. In addition to polarity, the resins can be classified into different types according to their average pore sizes distribution and surface areas (Wang et al., 2001; Tu et al., 2004)

Most commercially available resins always contain non-reacted monomers, pore-forming agents and cross-linking agents remaining trapped within the pore structure after polymerization. These organic residues must be removed before use as they are toxic and affect the adsorption capacity of the resins. A common pretreatment method is to extract the resins by absolute ethanol for 8 hours in a Soxhlet apparatus and then dry the resins under vacuum at 325K for 3 hours before use (Wang et al., 2001; Tu et al., 2004).

The resin will decrease its adsorption capacity or may be contaminated after a period of using. Thus, the resin needs regeneration. The method is to add 3%-5% hydrochloric acid to a level 10 cm above the resin layer in the column and immersed it for 2-4 hours. The resin is then rinsed by 3-4 bed volumes of hydrochloric acid and by distilled water until the pH of the effluent becomes neutral. Then 3%-5% sodium hydroxide is added to immerse the resin for 4 hours. After that, the resin is rinsed by 3-4 bed volumes of sodium hydroxide and finally by distilled water until pH of the effluent becomes neutral (Tu et al., 2004).

2.3.2 Adsorption mechanism

Adsorption of organic molecules by macroporous resins is attributed to two types of molecular interactions including van der Waals forces and hydrogen bonding. Both of them are electrostatic attraction between dipoles, i.e. the attraction between the positive end of one molecule and the negative end of another molecule. There are three types of dipoles – permanent dipole, instantaneous dipole and induced dipole. Permanent dipole exists in all polar molecules as a result of the difference in the electronegativity of bonded atoms. Instantaneous dipole is a temporary dipole that exists as a result of fluctuation in the electron cloud. Induced dipole is a temporary dipole that is created due to the influence of a neighbouring dipole (which may be a permanent or an instantaneous dipole).

Van der Waals force is a general term. It consists of two types of intermolecular attractions – dispersion forces (also known as London forces) and dipole-dipole attractions. The origin of van der Waals dispersion forces is temporary fluctuating dipoles. This dispersion forces exist in all molecules. Attractions are electrical in nature. In a symmetrical molecule like hydrogen, it seems that no electrical distortion to produce positive or negative parts. But it is only true on average. The electron cloud distribution is generally symmetrical around the nucleus. However, the

electrons are mobile. As the instant mobility of the electron cloud, its position fluctuates all the time. At any particular instant, it is likely to be concentrated on one end of the molecules, making that end slightly negative (δ^-). The other end will be temporarily shortage of electron and so becomes slightly positive (δ^+). Thus the molecule possesses an electric dipole (a polarity) at that particular instant. An instant later the electrons may move to the other end, reversing the polarity of the molecule.

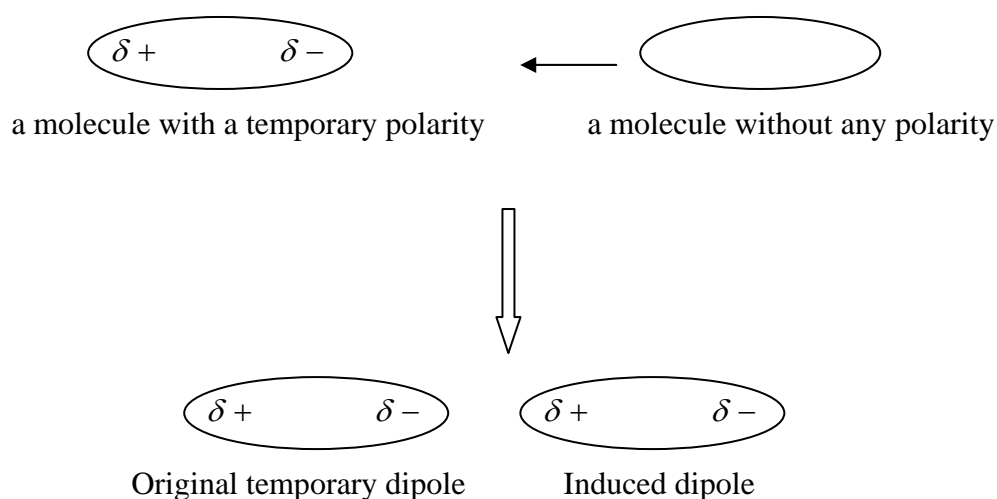


Figure 2.2 The formation of induced dipole.

Fig.2.2 shows the formation of induced dipole. When the right hand molecule which is entirely non-polar at that moment approaches, its electrons will tend to be attracted by the slightly positive end of the left hand one which has a temporary polarity (instantaneous dipole). This sets up an induced dipole in the approaching molecule, which is orientated in such a way that the δ^+ end of one is attracted to the δ^- end

of the other. Then, the two molecules interact with each other. Thus, the intermolecular attractions are created by these temporary dipoles.

The other type of van der Waals forces is dipole-dipole interactions. It exists only in polar molecules. A molecule like HCl has a permanent dipole because chlorine is more electronegative than hydrogen. These permanent, in-built dipoles will cause the HCl molecules to attract each other rather more than they attract, rely only on dispersion forces. All molecules experience dispersion forces. Dipole-dipole interactions are not an alternative to dispersion forces - they occur in addition to them.

The attraction between the lone pair electrons of the electronegative atom and slightly positively charged hydrogen atom of another molecule is called hydrogen bond. It is much weaker than the covalent bond but much stronger than van der Waals forces.

There are two essential requirements for the formation of a hydrogen bond:

- 1) a hydrogen atom must be directly bonded to a highly electronegative atom e.g. F, O and N, causing the hydrogen atom acquires a slightly positive charge; and

2) an unshared pair of electrons (lone pair electrons) on the electronegative atom.

The ammonia, water and hydrogen fluoride molecules acquire this bonding.

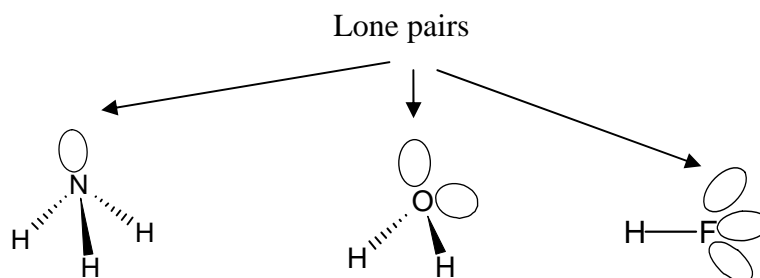


Figure 2.3 The lone pair electrons on ammonia, water and hydrogen fluoride molecules.

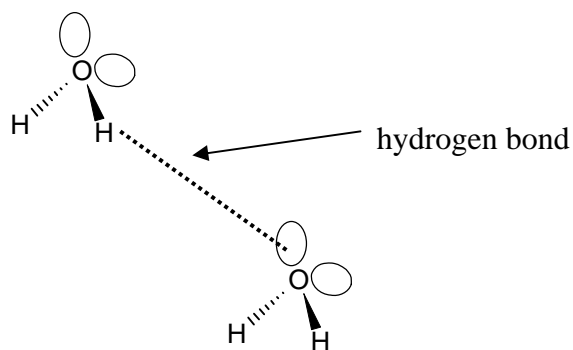


Figure 2.4 The hydrogen bonding between two water molecules.

Both bonding forces are weaker than the electrostatic attractions present in ion-exchange resins, so regeneration of such resins is easier. For hydrophobic (non-polar) resins, they adsorb certain organic molecules from aqueous solutions via van der Waals forces interaction between hydrophobic parts of organic molecules and

the resins. For hydrophilic (polar) resins, they adsorb certain organic molecules by mainly hydrogen bonding interaction. Under the principle of “like dissolve like”, the non-polar resins are particularly effective for adsorbing non-polar molecules from polar solvents e.g. water. Conversely, the highly polar resins are more effective for adsorbing polar molecules from non-polar solvents e.g. hydrocarbons.

In addition to the polarities, the pores structures such as surface areas and average pore-size distributions of the resins also play important roles in adsorption. The resins are porous spherical beads and have certain pores structures suitable for diffusion of certain organic molecules. When a solution is allowed to contact with resins, smaller organic molecules can penetrate into the beads by diffusing through the pores. On the contrary, organic molecules that are larger than the pore size cannot penetrate into the inside of beads. Consequently, such organic molecules may not be adsorbed on the resins (this phenomenon is so-called molecular sieving effect).

In general, adsorption of organic molecules by macroporous resins is the combination of molecular interactions and molecular sieving effect. The most appropriate type of resin should be selected according to the polarity, pore size of resin and the polarity, molecular size of the target compounds.

2.3.3 Commercially available resins

Owing to the property of tailor make, the resins display a wide range of adsorption behavior and have practical applications in diverse fields. The major application of the resins is in industrial wastewater treatments. The resins are widely used in removing organic pollutants such as phenol, chlorinated pesticides, benzenes, ketones, phenylenediamine, aniline, indenes, alkyl anphthalenes, etc. from industrial wastewater. Some valuable organic molecules e.g. phenols in the waste streams could be recovered from the resins by solvent elution since porous resin adsorption is a reversible process (Xu et al., 2002). The other applications include separation of valuable components from plant extracts or natural products, purification and recovery of fermented products e.g. antibiotics, enzymes, peptides and proteins for pharmaceutical intermediates and food additives (Li and Li, 2005).

Three common commercially available macroporous adsorption resins are introduced. They include Amberlite™ XAD™ series (Rohm and Haas Company., America), Diaion HP20 and HP21 (Mitsubishi Chemical Industries Ltd., Japan) and HPD series (HeBei CangZhou Bon Chemical Co. Ltd., China).

A. Amberlite™ XAD™ series

Amberlite™ XAD™ absorbent resins are widely used in treatment of wastewater, purification and recovery of plant extracts and fermented products such as antibiotics, enzymes and peptides. The series are XAD-4, XAD-16, XAD-1180, XAD-1600 (both are polystyrene DVB), XAD-7HP (aliphatic ester) and XAD-761(formophenolic). They have different particle diameters, pore diameters and surface areas. The particle diameters range from 0.35 to 0.76 mm, the pore diameters range from 100 to 600Å and the surface areas range from 200 to 800 m²/g. XAD-4 is mainly applied in wastewater treatment to remove many organic pollutants. It could also recover enzymatic synthesis of antibiotics-ampicillin by adsorption and then desorption (Xu et al., 2002).

B. Diaion HP-20 and HP-21

The resins are polystyrene DVB copolymer. Both have approximate 600 m²/g surface areas and 0.5 mm mean particle diameters. HP-20 has pore radius 200-300Å while HP-21 has pore radius 100-120Å. They are widely used in a broad range of applications, including the purification of amino acids, sugars, enzymes, extraction of antibiotic from fermentation broth and separation of valuable compounds from plant extracts. A previous research demonstrated that Diaion HP-20 packed in a column

as a first chromatographic procedure was used to isolate an antibiotic from the culture filtrates of *Pseudomonas fluorescens* Strain MM-B16 (Jung et al., 2003).

C. HPD series

The series are HPD100, HPD300, HPD400, HPD450, HPD500, HPD600, HPD700 and HPD800. HPD100, HPD300 and HPD700 are non-polar resins. HPD400 and HPD450 are medium polar resins. HPD500, HPD600 and HPD800 are polar resins. They have 0.3-1.25 mm particle diameters, 233-1265 m²/g surface area and 50-80Å average pore diameters. They are widely used in purification of antibiotics, vitamins, amino acids and proteins. In recent years, they have been widely applied in separating active ingredients such as saponins, alkaloids and flavones from crude extracts of TCMs. They have significant effects on purification, separation and recovery of active ingredients in several TCMs such as ginsenosides in *Radix Ginseng*, notoginsenosides in *Radix Notoginseng*, gypenosides in *Gynostemmatis Pentaphylli*, steviosides in *Folium Steviae*, glycyrrhizins in *Radix Glycyrrhizae*, Ginkgolides in *Folium Ginkgo*, flavones in *Fructus Hippophae*, Puerarin in *Radix Puerariae*, saponins in *Radix Astragali*, isoflavones in Soybeans, tea polyphenol and some natural pigments. A literature showed that HPD300 packed in a column could be used to separate and purify total saponins from *Cornus Officinalis* (Wu et al., 2003). The other research

report showed that HPD300 could separate and purify a well-known multifunction plant hormone, abscisic acid. The purity of abscisic acid could reach around 63% (Zheng et al., 2003). The non-polar HPD100 performed better to purify total saponins in *Polygala Fallax Hemsl* (Zhong et al., 2004). The HPD600 was the most suitable resin to separate red pigment in *Parthenocissus Tricuspidate Planch* in a research (Dong et al., 2004). The HPD400 performed better to separate crocin in *Fructus gardeniae* (Wang et al., 2004).

2.4 Isolation and purification of active ingredients of TCMs by MAR

In the past two decades, MAR has been widely used in separation and purification of active ingredients in TCMs. In 1979, Fung and co-workers first reported using MAR to separate gastrodin from *Gastrodia Elata* (Fung et al., 1979).

MAR has been successfully separated and purified saponins (Zheng et al., 2002; Li et al., 1994; Jin et al., 1999; Liu et al., 2001), flavonoids (Ma et al., 1997; Pan et al., 1999; Gao et al., 2001; Feng and Gu, 2003; Lu et al., 2004) and alkaloids in TCMs, camptothecin (Zhang et al., 1995) and other organic compounds such as Perilla pigment (Zhang and Chen, 1999), shikonin (Meng and Zhang, 1999) and tea polyphenols (Zhang et al., 2001; Dong et al., 2002).

The general procedures for investigating the separation and purification of target ingredients in TCMs by MAR are divided into two main steps– static experiments and dynamic experiments. Commonly, static experiments are done before dynamic experiments.

2.4.1 Static experiments

Static experiments are carried out in a rotary shaker in order to select the appropriate resin; determine the adsorption isotherm, adsorption thermodynamic and adsorption kinetics and investigate the factors affecting adsorption capacity of resin such as pH of sample solution, temperature and ionic strength.

2.4.1.1 Selection of the resin

Adsorption capacity and adsorption efficiency are commonly used to evaluate the adsorption performance of the resins.

The adsorption capacity is defined as follows (Zhang et al.,2006):

$$Q = \frac{(C_o - C_e)V}{m} \quad (1)$$

where Q – adsorption capacity (mg/g resin)

C_o – initial concentration of target ingredients (mg/ml)

C_e – equilibrium concentration of target ingredients (mg/ml)

V – volume of sample solution (ml)

m – mass of resin (g)

The adsorption efficiency is calculated as follows:

$$\text{Adsorption efficiency} = \frac{C_o - C_e}{C_o} \times 100\% \quad (2)$$

Besides, the desorption efficiency is used to evaluate the desorption performance of the resins, and is specified as follows:

$$\text{Desorption efficiency} = \frac{m_s}{m_r} \times 100\% \quad (3)$$

where m_s = mass of target ingredients desorbed in solvent (mg)

m_r = mass of target ingredients adsorbed on resin (mg)

The resin with the relatively highest adsorption capacity, adsorption efficiency and desorption efficiency for target ingredients is the most appropriate resin for the separation and purification process.

2.4.1.2 Determination of adsorption isotherms

Langmuir and Freundlich isotherm are the two most common equilibrium models to exhibit the adsorption systems (Frank, 1985).

Langmuir isotherm refers to monolayer adsorption and is expressed by the equation

(Warren et al., 2005):

$$Q_e = \frac{Q_m K_L C_e}{1 + K_L C_e} \quad (4)$$

where Q_e – the equilibrium adsorption capacity (mg/g resin)

Q_m – maximum adsorption capacity (mg/g resin)

K_L – Langmuir constant (ml/mg)

C_e – equilibrium solute concentration (mg/ml)

Freundlich isotherm refers to multilayer adsorption and is expressed by the equation:

(Warren et al., 2005)

$$Q_e = K_F C_e^{1/n} \quad (5)$$

where Q_e – the equilibrium adsorption capacity (mg/g resin)

C_e – equilibrium solute concentration (mg/ml)

K_F – Freundlich constant

$1/n$ – the Freundlich parameter

2.4.1.3 Determination of adsorption kinetic

The adsorption rate of the resin for target ingredients is also an important factor to evaluate the performance of the resin. A graph of adsorption kinetic can be obtained by measuring adsorption capacity at different time interval.

2.4.2 Dynamic experiments

Dynamic experiments are carried out by packing the resin selected from the static study into a column.

There are four steps for dynamic experiments. (Thurman et al., 1998)

Step 1 – conditioning the solid phase sorbent (resin)

A solvent is first passed through the sorbent to wet the packing material and to solvate the functional groups of the sorbent. Ethanol is the typical conditioning solvent, which is followed with distilled water.

Step 2 – loading sample solution into the column

It is a retention or loading step. A definite volume of sample solution is applied to the column either by gravity feed or pumping aspirated by vacuum. During this retention step, the analyte is accumulated on the sorbent. Some of the matrix components may

also be retained and others may pass through, thus partial purification on the analyte is achieved.

Step 3 – eluting the interferences

The column is rinsed to eluate the interferences. This will remove the sample matrix from the interstitial spaces of the column, while retaining the analyte. The rinsing solvent is usually distilled water.

Step 4 – eluting the analyte

The analyte is eluted from the sorbent with an appropriate solvent that is specifically chosen to disrupt the analyte – sorbent interaction, resulting in elution of the analyte.

Dynamic experiments are carried out to investigate the effect of feed flow rate on the breakthrough point of the breakthrough curve and the effects of eluent composition and flow rate on the desorption performance of the column.

2.4.3 Factors affecting the adsorption of active ingredients in TCMs

The adsorption capacity of MAR for active ingredients in TCMs is dependent upon a number of factors. These include the characteristics of (a) active ingredients, such as

polarity, molecular weight, solubility, etc.; (b) sorbents, such as surface area, pore size distribution, polarity, etc.; (c) operating conditions, such as temperature, pH, flow rate, feed concentration, ionic strength, etc. (Frank, 1985).

2.5 Application of MAR in previous research

2.5.1 Natural products

Lu and co-workers studied the adsorption characteristics of the soybean isoflavones on three macroporous resins AB-8, NKA-9 and DM-301 in order to separate and purify the isoflavones. Based on the results of adsorption isotherms and adsorption kinetics experiments, AB-8 was chosen as the best resin for adsorption of isoflavones (Lu et al., 2004).

In a study, eight resins including LSA-21, LSA-30, LSA-40, D101, HP-10, H107, XAD-1 and XAD-3 were used to compare their performances in adsorbing and desorbing flavonoids in *P.sibiricum Redoute*. The experimental results showed that LSA-30 resin possessed the highest adsorption and desorption capacity (Qi et al., 2005).

In the above studies, both resins applied were not in a series. In addition, their surface polarities and pore structures were not mentioned. Then, the effects of surface polarities and pore structures on the adsorption performance of the resins were not investigated. As a result, it could not conclude a relationship between the physical and chemical properties of the resin and its adsorption capacity.

2.5.2 Saponins in TCMs

Jin and his research group chose D-101 macroporous resin to extract and purify saponins in *Tribulus terrestris L.* The effects of different eluent composition on the desorption performance of the column in term of recovery yield were investigated. The eluent including 20%, 40%, 60%, 80% and 95% aqueous ethanol were used to eluate the loaded column in an isocratic and individual way. 80% aqueous ethanol was found to be the most proper eluent as the recovery yield was the highest (Jin et al., 1999).

In a previous research, the adsorption capacity and service life of D-101 macroporous resin for ginsenoside were studied. The results showed that the adsorption capacity of D-101 for ginsenoside is large (ginsenoside: D-101 resin = 1:10). Besides, the column

was able to retain nearly 50% of the original adsorption capacity after four successive adsorption/desorption cycle (Zheng et al., 2002).

Liu and his colleagues carried out experiments to study the purification of *Panax Notoginseng* saponins by D-101 macroporous resin. The step-gradient elution program (200 ml 0%, 100 ml 30%, 100 ml 50% and 100 ml 70% aqueous ethanol) was applied to eluate the loaded column. The results showed that around 90% of total saponins were desorbed in 30% and 50% aqueous ethanol. The elution program was modified, the new program was 100 ml distilled water followed by 100 ml 50% aqueous ethanol. The purity obtained was around 70% (Liu et al., 2001).

Referring to the above researches, it was observed that only one single resin was applied. It came across the same limitations as mentioned before. The limitations are the findings could not give a guideline for selecting the appropriate resin for adsorption and relate the resin structures to the adsorption capacity. In addition, the effects of experimental parameters such as temperature, initial saponins concentration, adsorption time and pH of sample solution on adsorption were not investigated. For evaluating the desorption performance, only recovery yield or purity was considered. It could not give a comprehensive evaluation.

So far, no information is found in the published literatures concerning the adsorption of saponins on a series of resins and the comprehensive operation for column adsorption. Therefore, the main objective of this study was to evaluate the adsorption characteristics of saponins on the HPD series resins. The series resins can be classified into polar, medium polar and non-polar and they are different in resin structures. Thus the adsorption capacities of the resins affected by surface polarity and resin structures could be investigated. In addition, the effects of experimental parameters mentioned before on adsorption were studied.

In dynamic experiments, the effects of operating parameters such as feed flow rate, feed concentration and bed depth on the adsorption performance of the column were determined. Besides, different step-gradient elution programs were applied to study their effects on the desorption performance of the column in terms of purity, recovery yield and concentration ratio.

This research could provide useful guideline for the selection of the proper resins for the preparative separation of active ingredients from herbal extracts in general as well as the design and operation of adsorption column systems for separating and purifying active ingredients of the Chinese medicinal herbs.

3. Materials and methods

3.1 Reagents

The raw Chai Hu was purchased from Zhixin Medicine Co. Limited (PR China). HPLC grade acetonitrile and methanol were obtained from Tedia company, Inc. (USA). Analytical grade ethanol was supplied from International Laboratory (USA). Saikosaponin a (ssa), saikosaponin c (ssc) and saikosaponin d (ssd) standards were obtained from Wako Pure Chemical Industries, Ltd. (Japan). All solutions were filtered through 0.45 μm nylon syringe filter (Chellesson Scientific Instruments Company) before HPLC analysis. Freshly deionized water prepared by a Millipore Milli-Q (BiocelTM A10TM, Millipore SAS, France) was used in the experiments.

3.2 Adsorbents

Macroporous resins including HPD100, HPD300, HPD400, HPD450, HPD500, HPD600, HPD700 and HPD800 were obtained from CangZhou Bon Chemical Co. Ltd. (HeBei, PR China). Their physical properties are listed in Table 3.1. The detailed chemical structures and arrangement of functional groups of the eight resins are not known. The physical properties obtained are based on the information provided by the manufacturers. The surface area and the pore distribution of the adsorbent resins were measured by BET and BJH methods respectively using a Micrometics ASAP-2010

automatic surface analysis instrument (Micromeritics Instrument, Norcross, USA). The adsorbent resins were pre-treated to remove the monomers and pore forming agents trapped inside the pores during the synthesis process. Prior to use, the resins were immersed in absolute ethanol for 24 hours. Then, the resins were filtered and washed with appropriate amount of distilled-deionized water to remove any residual ethanol.

Table 3.1 Physical properties of HPD series resins

Property	Polarity	BET surface area (m ² /g)	Average pore diameter (nm)	Average particle size (mm)
HPD100	Non-polar	783.4 ± 1.6	6.9	
HPD300	Non-polar	1264.8 ± 2.5	6.0	
HPD400	Moderate polar	701.4 ± 1.1	8.3	
HPD450	Moderate polar	543.1 ± 1.2	7.7	0.30-1.25
HPD500	Polar	887.9 ± 1.9	7.3	
HPD600	Polar	255.2 ± 0.6	7.1	
HPD700	Non-polar	609.3 ± 1.4	6.7	
HPD800	Moderate polar	233.3 ± 0.5	4.8	

3.3 Preparation of crude Radix Bupleuri extracts

30 g of Chai Hu was minced and ground into powder by a disintegrator and extracted with 360 ml of a solution of ethanol/water (65:35, v/v) by sonication in an ultrasonic bath for 2 hours. The extraction solution was filtered. The filtrate was concentrated to one tenth of the original volume by removing the ethanol solvent with a rotary evaporator (Shanghai, RP China) at 36°C.

3.4 HPLC analysis of saikosaponins a, c and d

Quantifications of ssa, ssc and ssd concentration were carried out by a Agilent 1100 series HPLC system equipped with a variable wavelength UV-visible detector and a Hypersil ODS-C₁₈ reversed-phase column (200 mm X 4.6 mm, I.D., 5 µm). The UV detector was set at the wavelength of 210 nm. The column temperature was maintained at room temperature (20-25°C). Gradient elution was employed by varying the proportion of acetonitrile (solvent A) and water (solvent B). The gradient program was: 0-10 min, 72% of B; 10-18 min, 72-62% of B; 18-28 min, 62-58% of B; 28-35 min, 58% of B; 35-37 min, 58-72% of B. The flow rate was maintained at 1ml/min throughout the run and the sample injection volume was 20 µl. The retention time of ssa, ssc and ssd were 22.8 min, 17.1 min and 32.8 min respectively. The HPLC chromatogram of ssa, ssc and ssd standards is shown in Fig. 3.1.

The calibration curve based on standard solution of ssa, ssc and ssd exhibited good linearity over the range of 20 - 100 µg/ml. It is shown in Fig.3.2. The regression line for ssa, ssc and ssd were $y_a = 288.46x - 17.245$ ($R^2=0.990$), $y_c = 210.37x - 9.8425$ ($R^2=0.996$) and $y_d = 221.7x - 6.9437$ ($R^2=0.995$) respectively, where y_i referred to the peak area of component i and x referred to the concentration (µg).

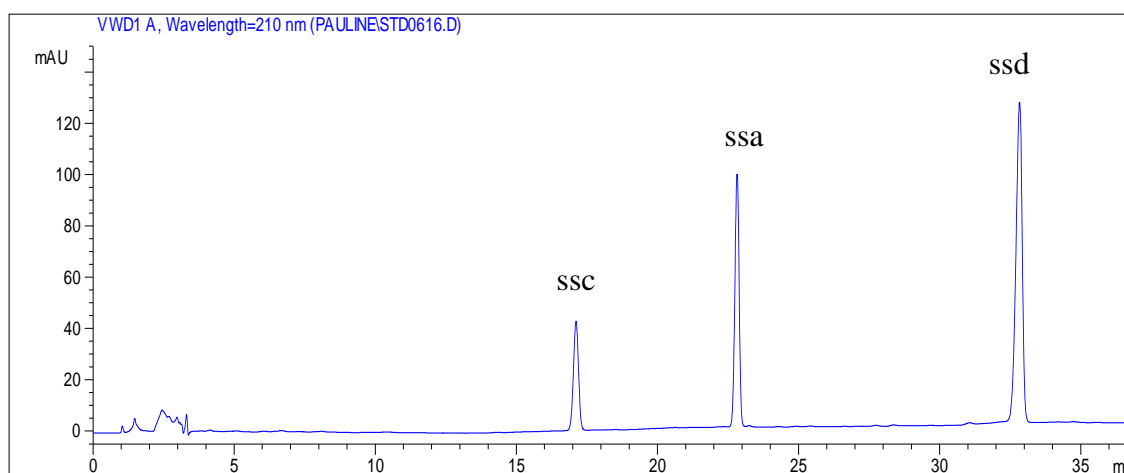


Figure 3.1 HPLC chromatogram at wavelength 210 nm of ssa, ssc and ssd standards.

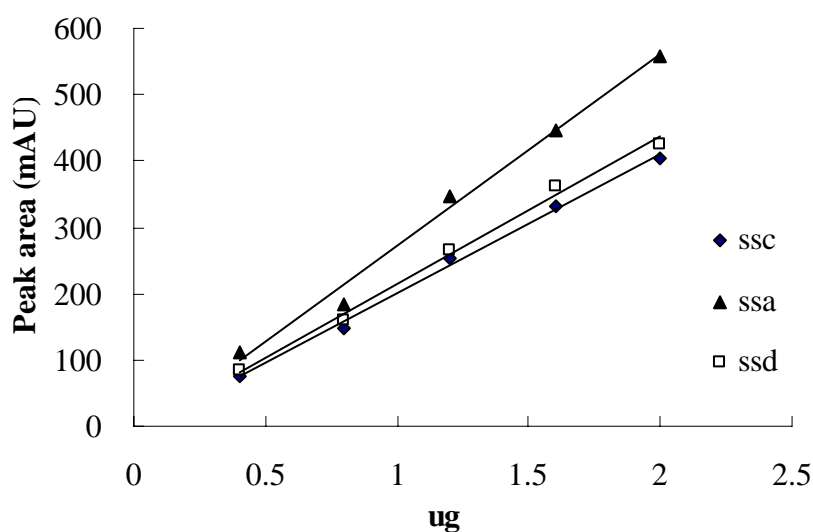


Figure 3.2 Calibration curve for saikosaponins standards.

4. Static study

4.1 Experimental section

4.1.1 Static adsorption

In each static experiment, 100 ml of Chai Hu extract of same initial concentration of total saikosaponins were added to 2.00 ± 0.01 g resin in a 250 ml conical flask at 298.0 ± 0.5 K. The pH of the sample solution was 5.0 ± 0.1 . One flask with same dosage of sample solution but no resin was used as control. The flasks were completely sealed and shaken in a shaker under 150 rpm. The static adsorptions were run continuously for 24 hours. Then, the equilibrium concentrations of saikosaponins and the adsorption capacities were determined. The set-up for static adsorption is showed in Picture 4.1.



Picture 4.1 The experimental set-up for static adsorption.

The adsorption capacity was calculated as follows:

$$Q_e = (C_o - C_e) \frac{V}{W} \quad (1)$$

$$E = \frac{(C_o - C_e)}{C_o} 100\% \quad (2)$$

where Q_e is the adsorption capacity at adsorption equilibrium (mg/g resin); E is the adsorption ratio (%), which is the percentage of total adsorbate mass being adsorbed after reaching equilibrium; C_o and C_e are the initial and equilibrium concentrations of adsorbate in the solutions respectively (mg/ml); V is the volume of the initial sample solution (ml) and W is the weight of the treated adsorbent resins (g).

Experiments were also conducted to investigate the effects of the experimental parameters such as temperature, initial saikosaponins concentration and pH of sample solution on the adsorption.

4.1.2 Static desorption

Each resin with adsorbed saikosaponins was introduced into a 250 ml conical flask containing 100 ml aqueous ethanol (35:65, v/v). The flasks were entirely sealed and

shaken at 298.0 ± 0.5 K under 150 rpm for 24 hours. The desorption efficiency was calculated as follows:

$$\text{Desorption efficiency} = \frac{m_s}{m_r} \times 100\% \quad (3)$$

where m_s refers to the mass of target components desorbed in the solvent; m_r refers to mass of target components adsorbed on the resin.

4.1.3 Adsorption isotherms

The static adsorptions of Chai Hu extract were performed at three different temperatures, 288, 298 and 308 K. 1.00 ± 0.01 g each selected resin was introduced into a 250 ml conical flask containing 100 ml of Radix Bupleuri extract of different initial concentration of total saikosaponins (ranged from 26.17 to 52.38 mg/100ml). One flask with same dosage of sample solution but no resin was used as control. The flasks were completely sealed and shaken in a shaker at a pre-settled temperature under 150 rpm. The static adsorptions were run continuously for 24 hours. Then, the equilibrium concentrations of saikosaponins and the adsorption capacities were determined.

4.1.4 Adsorption kinetic

1.00 ± 0.01 g each selected resin was taken into a 250 ml conical flask containing 100 ml sample solution. The initial concentration of saikosaponins was 22.70 ± 0.17 mg/100ml. The flasks were shaken at 298.0 ± 0.5 K under 150 rpm for 24 hours. The samples were taken at different time intervals (0-24 hours) and the concentration of the saikosaponins was analyzed by HPLC.

The experiments mentioned above were replicated three times for each set conditions.

4.2 Results and discussion

4.2.1 Selection of adsorption resins

As mentioned before, adsorption capacity and adsorption efficiency were used to evaluate the adsorption performance of the resin. The desorption performance of the resin was evaluated by desorption efficiency. Eight resins namely HPD100, HPD300, HPD400, HPD450, HPD500, HPD600, HPD700 and HPD800 were used in this study.

The experiments were conducted at 298.0 ± 0.5 K using 100 ml adsorbate solution with pH 5.0 ± 0.1 and a fixed adsorbent dosage of 2.00 ± 0.01 g. The adsorption capacities Q_e , adsorption efficiencies and desorption efficiencies of eight resins for ssa, ssc and ssd were compared. The results were showed in the following Tables 4.1 and

4.2

Table 4.1 The adsorption capacities and adsorption efficiencies of individual saikosaponin on the eight resins.

Resin	Adsorption capacity (mg/g resin)			Adsorption efficiency (%)		
	ssc	ssa	ssd	ssc	ssa	ssd
HPD100	4.61 ± 0.21	13.35 ± 0.37	5.84 ± 0.27	83.59	84.16	47.89
HPD300	4.07 ± 0.48	12.85 ± 0.27	5.32 ± 0.39	79.69	79.32	43.32
HPD400	4.59 ± 0.21	11.70 ± 0.34	4.18 ± 0.65	87.48	77.42	38.10
HPD450	4.28 ± 0.51	11.36 ± 0.68	4.02 ± 0.72	77.96	75.81	35.81
HPD500	3.89 ± 0.32	11.42 ± 0.84	2.46 ± 0.09	74.03	73.78	20.81
HPD600	2.56 ± 0.77	7.82 ± 0.54	3.68 ± 0.27	53.63	50.41	29.62
HPD700	4.54 ± 0.45	11.35 ± 0.48	4.82 ± 0.54	84.01	78.45	41.77
HPD800	4.64 ± 0.32	11.20 ± 0.47	4.56 ± 0.42	84.23	74.91	39.95

Table 4.2 The adsorption capacities, adsorption efficiencies and desorption efficiency of total saikosaponins on the eight resins.

Resin	Total adsorption capacity (mg /g resin)	Total adsorption efficiency (%)	Total desorption efficiency (%)
HPD100	23.81 ± 0.50	71.40 ± 2.52	85.34 ± 3.66
HPD300	22.24 ± 0.67	66.25 ± 3.03	74.84 ± 5.33
HPD400	20.47 ± 0.76	65.35 ± 1.25	88.80 ± 5.07
HPD450	19.65 ± 1.11	62.04 ± 2.78	88.21 ± 4.21
HPD500	17.77 ± 0.90	53.11 ± 3.51	97.22 ± 0.81
HPD600	14.06 ± 0.98	43.16 ± 4.95	83.52 ± 5.74
HPD700	20.71 ± 0.85	66.13 ± 6.03	82.51 ± 6.13
HPD800	20.40 ± 0.71	64.23 ± 5.74	82.81 ± 2.49

Referring to the Table 3.1, the eight resins could be divided into three types. The non-polar resins are HPD100, HPD300 and HPD700. The moderate-polar resins include HPD400, HPD450 and HPD800. The polar resins are HPD500 and HPD600.

The results showed that adsorption of saikosaponins occurred on all hydrophobic (non-polar), moderate polar and hydrophilic (polar) resins but to different extent. The extent of adsorption relates to the interactions between the adsorbates and each adsorbent. The interactions responsible for adsorption include the van der Waals dispersion forces between hydrophobic parts of the organic molecule and the resin,

the hydrophobic bonding from the combination of the mutual attraction between hydrophobic groups of the organic molecules and their tendency to escape from an aqueous environment and hydrogen bonding (Kyriakopoulos et al., 2005). In addition, the chemical structure such as types of functional groups and physical properties e.g. porosity and surface area of the resin determine its adsorption capability (Wei et al., 2004).

In Table 4.2, it is observed that the adsorption capacities and efficiencies of saikosaponins on hydrophobic resins were the highest in comparison to those on moderate polar and hydrophilic resins. It indicated that hydrophobic resins adsorbed saikosaponins more effectively than moderate polar and hydrophilic resins. In all cases, van der Waals dispersion forces played the major role in adsorption of saikosaponins in all resins but the forces were the most dominant in the case of hydrophobic resins. The saikosaponins are hydrophobic molecules since they have hydrocarbon chains with a number of carbon atoms equal or higher than 42. Under the principle of “like attracts like”, the hydrophobic resins are particularly effective for adsorbing hydrophobic organic molecules from aqueous solvents e.g. water. Thus, the saikosaponins were more favorable for the adsorption on the hydrophobic resins.

As mentioned before, surface area is one of the factors affecting adsorption capacity

of a resin. For hydrophobic resins, the surface area of HPD300 ($1265 \text{ m}^2/\text{g}$) was much larger than those of HPD100 ($783 \text{ m}^2/\text{g}$) and HPD700 ($609 \text{ m}^2/\text{g}$). However, the difference in their adsorption capacities was not significant. Similar results could be observed in the case of moderate polar resins. It indicated that the effect of surface area on adsorption capacity was not significant.

The surface area of HPD500 ($888 \text{ m}^2/\text{g}$) was approximately 10% larger than that of HPD100 ($783 \text{ m}^2/\text{g}$), but the adsorption capacity of HPD100 was 30% greater than that of HPD500. It strongly suggested that the significant difference in adsorption capacity was not much related to the surface area but largely related to the hydrophobic property of the resin.

Besides the surface area, pore size of the resin may affect the adsorption capacity. The average pore diameters of all resins were approximately the same. All have around 5-8 nm pore diameter which was much larger than the estimated molecular size of saikosaponins (estimated molecular size of ssa, ssc and ssd were 0.61 nm, 0.64 nm and 0.61 nm respectively). Thus, saikosaponins could diffuse through the pores of all resins easily to the internal surface for adsorption. It indicated that the difference in adsorption capacity was not related to average pore diameters.

Regarding the desorption efficiency, nearly all resins except HPD300 had over 80% desorption efficiencies. It showed that over 80% saikosaponins adsorbed could be recovered by desorption. Thus, the desorption performance of the resins was acceptable.

Three type resins including hydrophobic HPD100, moderate polar HPD450 and hydrophilic HPD600 were selected for further study. The effects of different experimental parameters including temperature, initial saikosaponins concentration, pH and adsorption time on adsorption were investigated. In addition, the adsorption isotherms, kinetics and thermodynamic were determined.

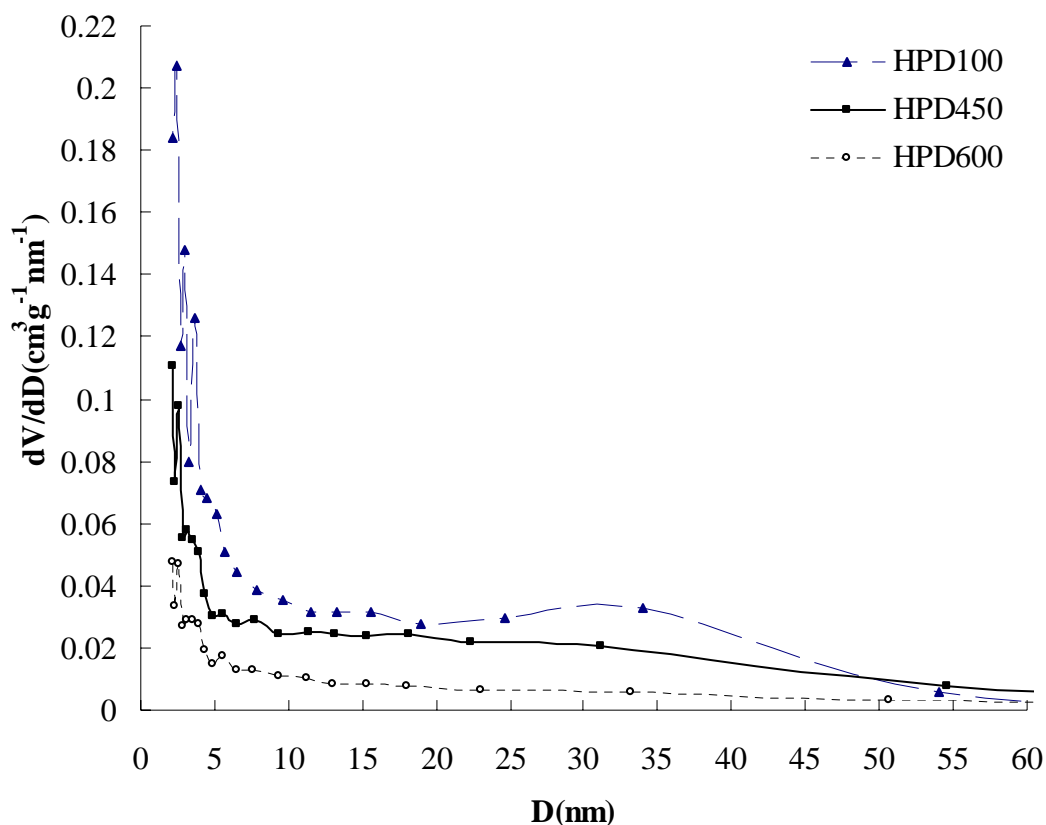


Figure 4.1 The plot of pore size distribution along pore diameter for HPD100, HPD450 and HPD600 resins.

4.2.2 Characterization of the polymeric adsorbents

The distribution of pore sizes of the three adsorbents HPD100, HPD450 and HPD600 measured by BET analysis are shown in Fig.4.1. All three resins exhibited wide distribution in pore sizes. ($D < 130$ nm for HPD450, $D < 120$ nm for HPD600 and $D < 100$ nm for HPD100, not shown). The mesopore (2 nm – 50 nm) dominated the pore structure of HPD100. The macropore ($D > 50$ nm) of HPD450 was more significant than that of HPD100 and HPD600 (not shown). Due to the limitation of BET analysis, distribution of micropore ($D < 2$ nm) could not be detected (Klaus et al., 1995). The

pore system is shown in Fig.4.2.

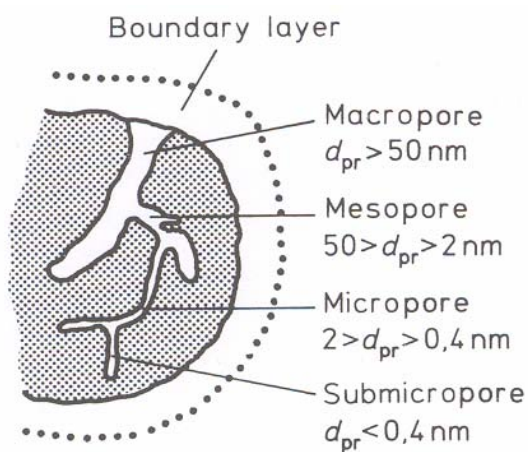


Figure 4.2 The pore system (cited from Klaus et al.,1995)

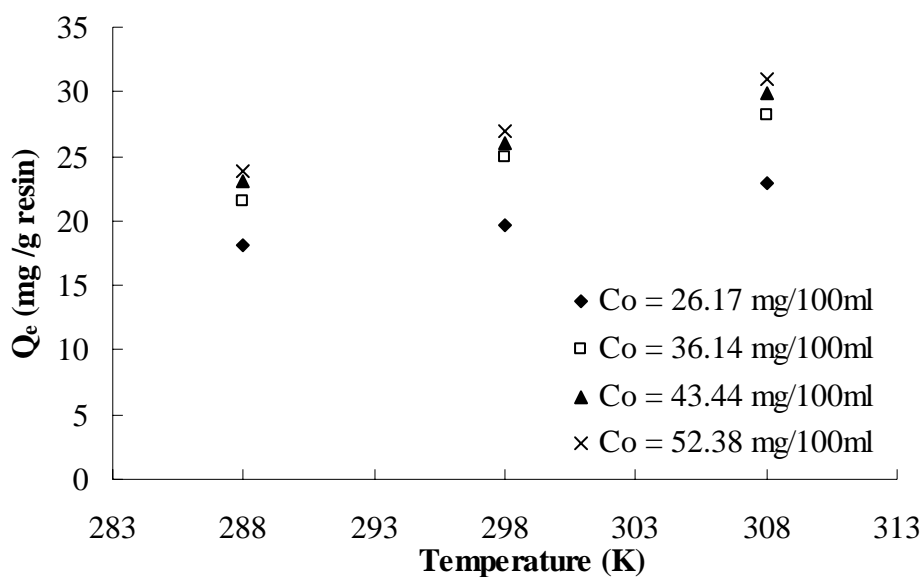


Figure 4.3 Effects of initial saikosaponins concentration and temperature on the adsorption capacity of HPD100 resin at conditions: adsorbent dosage $1.00 \pm 0.01 \text{ g}$, pH 5.0 ± 0.1 , agitation 150 rpm.

4.2.3 Effect of temperature

The effect of temperature on the saikosaponins adsorption on HPD100 resin was evaluated. Fig.4.3 shows the equilibrium adsorption capacity as a function of temperature. It is observed that adsorption increased with the increase of temperature from 288 K to 308 K for the same initial saikosaponins concentration. The result showed that the effect of temperature on saikosaponins adsorption was positive.

This phenomenon may be due to the fact that raising the temperature could lower the viscosity which facilitates the external transfer and diffusion of adsorbate within the adsorbent resin. In addition, the surface diffusion rate and intra-particle diffusion rate of saikosaponins could be increased at higher temperature as diffusion is an endothermic process. Thus, the adsorption was enhanced at higher temperature.

4.2.4 Effect of initial saikosaponins concentration

Four different initial saikosaponins concentrations were applied in this study to investigate the effect of initial saikosaponin concentration on adsorption. Fig.4.3 shows the adsorption increased with the increase of initial saikosaponins concentration from 26.17 mg/100ml to 52.38 mg/100ml at the same temperature.

The overall adsorption process of porous resins is composed of three consecutive mass transfer steps. First, the saikosaponins molecules diffuse from the bulk solution

through the boundary layer to the exterior surface of the adsorbent by molecular diffusion. Then, the saikosaponins molecules diffuse from the adsorbent surface into interior sites by pore diffusion. Finally, the saikosaponins molecules are adsorbed into the active sites at the interior surface of the adsorbent. Mass transfer occurs when a component in a mixture migrates in the same phase or from phase to phase because of a difference in concentration between two points.

The general molecular transport equation is shown as follows:

$$\text{rate of a transfer process} = \frac{\text{driving force}}{\text{resistance}}$$

This can be written as follows for molecular diffusion of mass:

$$\text{Fick's law: } J_{AZ} = -D_{AB} \frac{dC_A}{dZ}$$

where J_{AZ} is the molar flux of a component A in the Z direction due to molecular diffusion in Kgmol A/m^2 , D_{AB} is the molecular diffusivity of the molecule A in B in m^2/s , C_A is the concentration of A in Kgmol/m^3 and Z is the distance of diffusion in m.

Referring to the Fick's law equation, concentration is the driving force for mass

transfer. It indicated that the initial concentration of adsorbate is an important driving force to overcome the mass transfer resistances between the aqueous and solid phases. Hence, a higher initial saikosaponins concentration would enhance the adsorption process.

In Fig.4.3, it is observed that the difference in adsorption capacity was not significant when the initial saikosaponins concentration was over 36.14 mg/100ml. It may be due to the limitation of active sites for adsorption of the porous resins. The active sites in the interior surface of the resins were nearly used up and reached saturation. Therefore, the resins would not adsorb much even the initial saikosaponins concentration increased.

4.2.5 Effect of pH

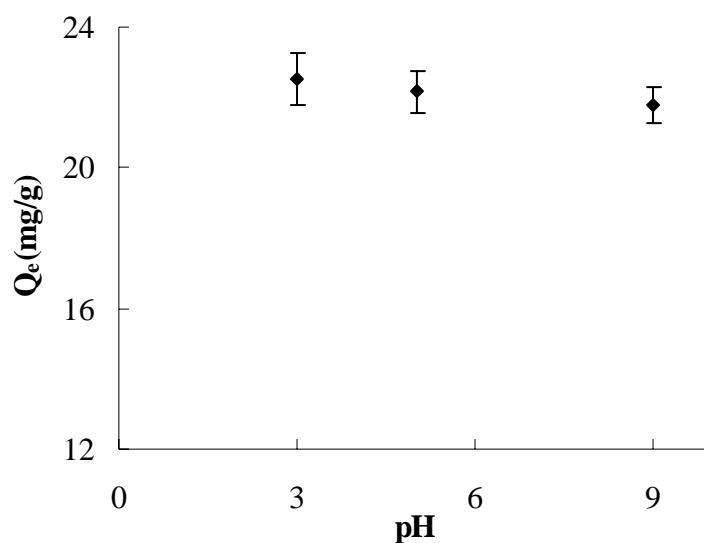


Figure 4.4 Effect of pH on saikosaponins adsorption on HPD100 at conditions: adsorbent dosage 1.00 ± 0.01 g, agitation 150 rpm.

The effect of pH on adsorption of saikosaponins on HPD100 was studied at a temperature of 298.0 ± 0.5 K by varying the initial pH of 28.00 mg/100ml of saikosaponins solution for a fixed adsorbent dosage of 1.00 ± 0.01 g.

Fig.4.4 illustrates the extent of adsorption on HPD100 changed with the solution pH including pH 3.0, pH 5.0 and pH 9.0. It clearly showed that the extent of adsorption did not change significantly with different pH values. As mentioned before, the extent of adsorption relates to the interactions between the adsorbates and adsorbent surfaces. In the case of HPD100, the interaction responsible for adsorption is mainly the van der Waals dispersion forces between hydrophobic parts of the organic molecule and

the resin.

The following equation shows the relation between solution pH and pKa of acid.

$$\text{pH} = \text{pKa} + \log \frac{[\textit{ionic form}]}{[\textit{molecular form}]} \quad (4)$$

where Ka is a dissociation constant of acid and $\text{pKa} = -\log \text{Ka}$.

Referring to the equation (4), if the solution $\text{pH} > \text{pKa}$ of acid, the acid is in ionic form. If the solution $\text{pH} < \text{pKa}$, the acid is in molecular form. In the pH range studied (from pH 3.0 to pH 9.0), the saikosaponins molecules were in molecular forms rather than the ionic forms as the pKa of saikosaponin a is 12.82 ± 0.70 which is larger than the pH range studied. Therefore, the hydrophobic natures of the saikosaponins molecules did not change much in the pH range studied. Thus, the van der Waals dispersion forces responsible for the interactions as well as the extent of adsorption were not affected.

4.2.6 Adsorption isotherms

The adsorption isotherms express the relationships between equilibrium concentrations of the adsorbates in the solid phase (Q) and liquid phase (C) at a fixed temperature. The concentration of adsorbates in liquid phase is expressed in mass units as mg/100ml. The concentration of adsorbates on the solid phase is given as mass adsorbed per unit mass of original adsorbent.

Figs.4.5-4.7 show the adsorption isotherms of saikosaponins on HPD100, HPD450 and HPD600 resins at three different temperatures, 288, 298 and 308 K. The adsorption data were analyzed using the Langmuir model and Freundlich model (Warren et al.,2005).

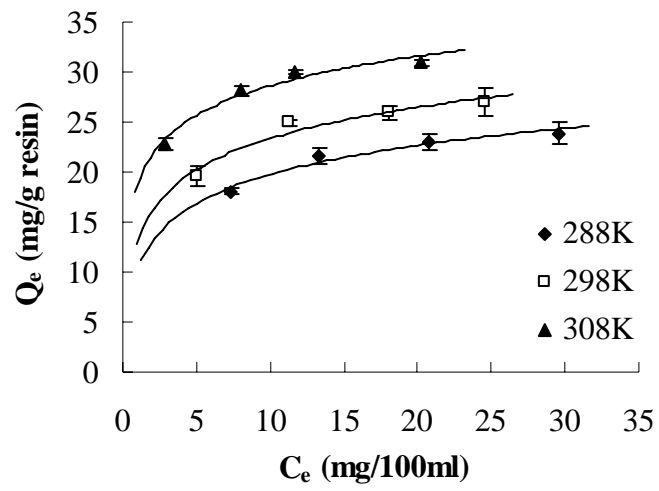


Figure 4.5 The adsorption isotherms of saikosaponins on HPD100 resin at different temperatures.

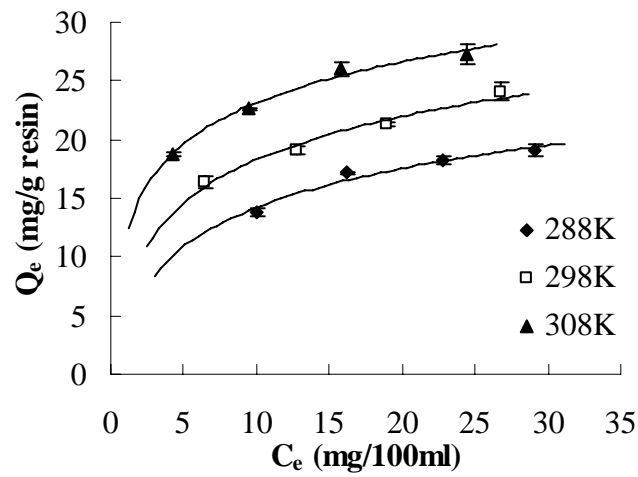


Figure 4.6 The adsorption isotherms of saikosaponins on HPD450 resin at different temperatures.

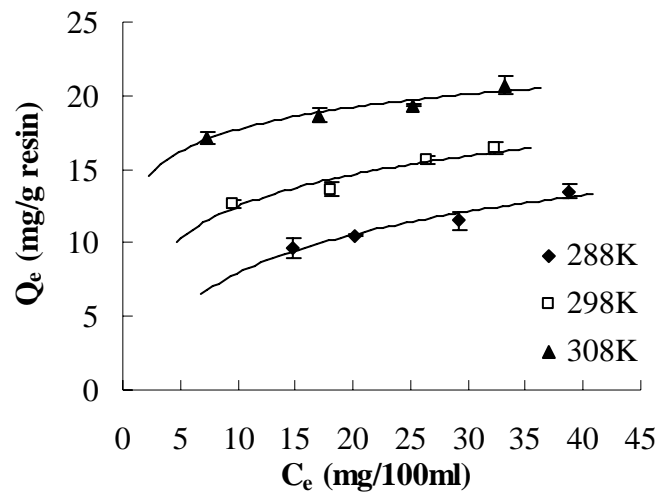


Figure 4.7 The adsorption isotherms of saikosaponins on HPD600 resin at different temperatures.

The Langmuir isotherm model is expressed as

$$\frac{Q_e}{Q_m} = \frac{K_L C_e}{1 + K_L C_e} \quad (5)$$

It is based on monolayer adsorption onto a surface with a finite number of identical sites. (constant heat of adsorption for all sites)

The Freundlich isotherm model can be expressed as

$$Q_e = K_F(C_e)^{1/n} \quad (6)$$

It is based on multilayer adsorption of adsorbates on the heterogeneous surface. This isotherm is assumed that the adsorption sites are distributed exponentially with respect to the heat of adsorption.

where K_L and K_F are the adsorption equilibrium constants of Langmuir and Freundlich models respectively. Q_m is a maximum adsorption capacity while $1/n$ is indicative of the energy or intensity of the adsorption. The adsorbent structure is shown in Fig.4.8.

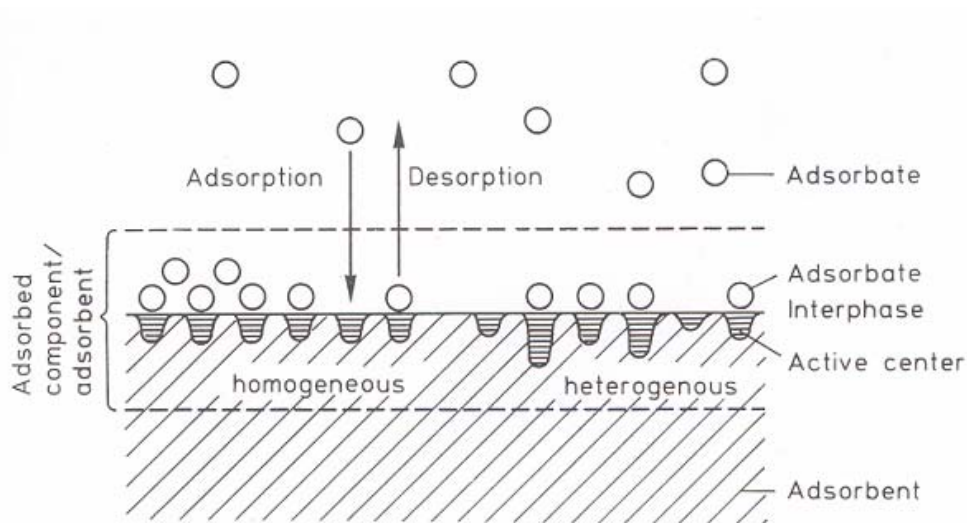


Figure 4.8 The adsorbent structure (cited from Klaus et al., 1995)

The linear forms of Langmuir model and Freundlich model equations are shown as follows:

$$\frac{1}{Q_e} = \frac{1}{Q_m} + \frac{1}{K_L Q_m C_e} \quad (7)$$

$$\ln Q_e = \ln K_F + \frac{1}{n} \ln C_e \quad (8)$$

The adsorption data was fitted to linear form of the Langmuir model equation (7). The Langmuir isotherms could be obtained by plotting $1/Q_e$ against $1/C_e$ as shown in Figs.4.9-4.11, which give the Langmuir isotherms for HPD100, HPD450 and HPD600 respectively. The intercept of regression lines at $1/Q_e$ axis gives $1/Q_m$ and the slope of lines gives $1/K_L Q_m$. The Q_m , K_L and r^2 (correlation coefficient) are listed in Table 4.3.

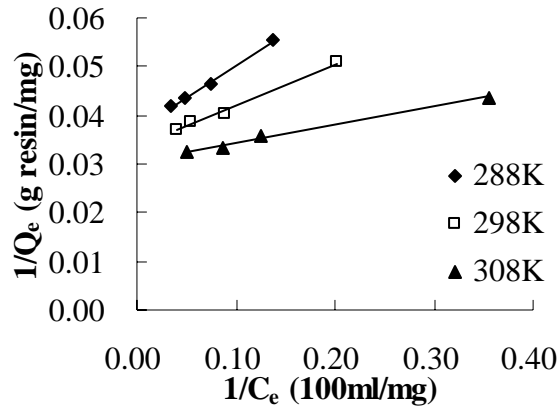


Figure 4.9 Langmuir isotherm for HPD100 (the plot of $1/Q_e$ against $1/C_e$).

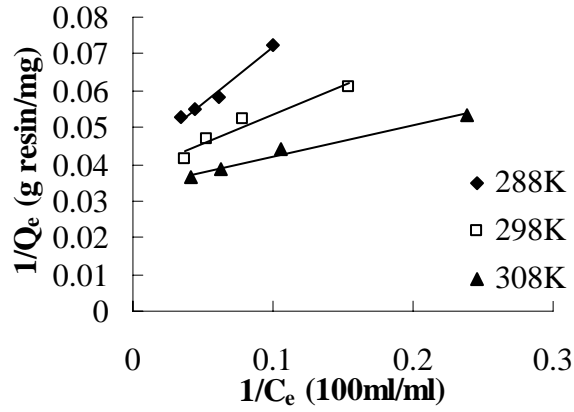


Figure 4.10 Langmuir isotherm for HPD450.

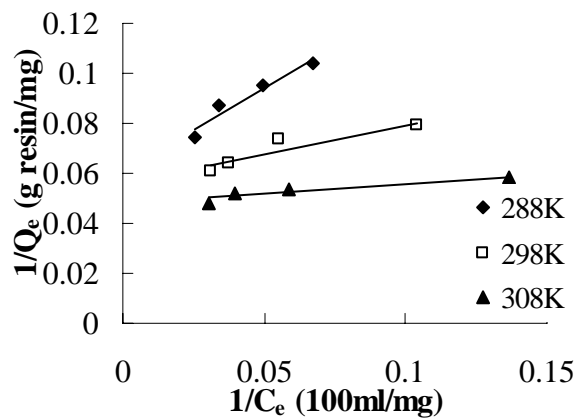


Figure 4.11 Langmuir isotherm for HPD600.

Table 4.3 Langmuir parameters

Adsorbents	Temperature (K)	Q _m (mg/g resin)	K _L (100ml/mg)	r ²
HPD100	288	26.95	0.28	0.996
	298	29.94	0.39	0.991
	308	32.79	0.81	0.997
HPD450	288	24.15	0.14	0.982
	298	26.39	0.24	0.944
	308	29.67	0.40	0.981
HPD600	288	16.53	0.09	0.934
	298	17.86	0.24	0.865
	308	21.01	0.59	0.895

The maximum adsorption capacity Q_m increased with increasing temperature indicating that adsorption was higher at a higher temperature. The increase in Q_m with increasing temperature was in agreement with the experimental results of temperature effect described before.

The adsorption data was also fitted to the linear form of the Freundlich model equation (8). Freundlich isotherms could be obtained by plotting $\ln Q_e$ against $\ln C_e$ as

shown in Figs.4.12-4.14, which give the Freundlich isotherms for HPD100, HPD450 and HPD600 respectively. The K_F and $1/n$ values are the intercept and the slope of the regression lines. The Freundlich parameters are summarized in Table 4.4.

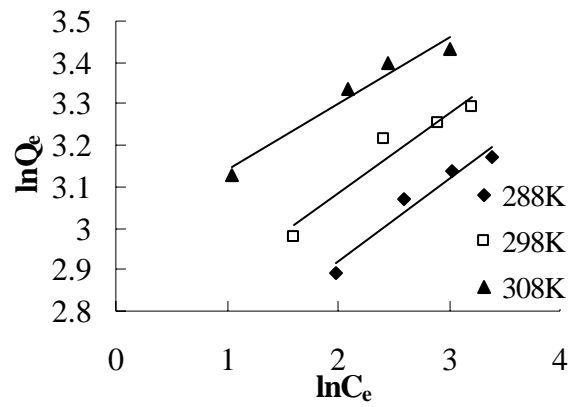


Figure 4.12 Freundlich isotherms for HPD100 (the plot of $\ln Q_e$ against $\ln C_e$).

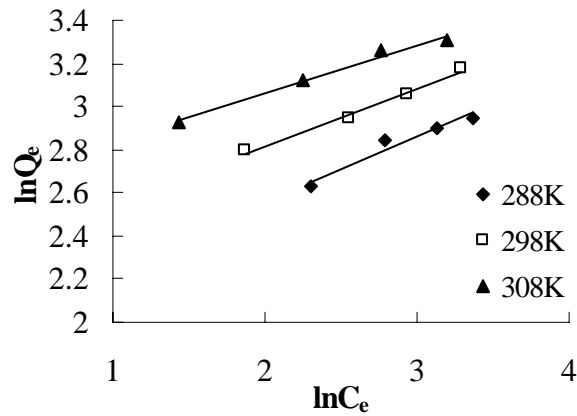


Figure 4.13 Freundlich isotherm for HPD450.

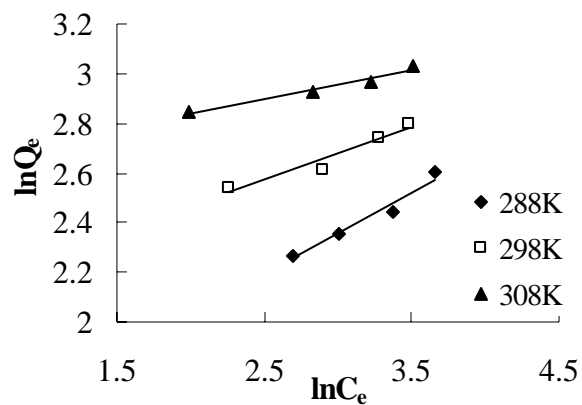


Figure 4.14 Freundlich isotherm for HPD600.

Table 4.4 Freundlich parameters

Adsorbents	Temperature (K)	K_F	n	r^2
HPD100	288	12.40	4.99	0.953
	298	14.76	5.12	0.934
	308	19.72	6.26	0.957
HPD450	288	7.19	3.38	0.943
	298	9.78	3.72	0.989
	308	13.74	4.51	0.985
HPD600	288	3.86	2.99	0.962
	298	7.60	4.61	0.937
	308	13.53	8.60	0.961

The correlation coefficient r^2 indicates the degree of correlation of adsorption process to the isotherm model. By comparing the r^2 obtained from the two isotherm models, the adsorption data of HPD100 fitted the best to Langmuir model since the r^2 of Langmuir isotherm were greater than 0.99 at the designated temperatures. The analysis of variance (ANOVA) on the r^2 was carried out. The results showed that the adsorption process on HPD100 can be classified as the type of monolayer at 95% significant level (refers to Appendix A.2 for details).

For HPD450 and HPD600, the r^2 obtained from the two isotherm models were further analyzed by ANOVA. The results showed that there is no significant difference between the r^2 of the two models at the designated temperatures. Please refer to Appendix A.2 for details. It indicated that the adsorption processes on HPD450 and HPD600 follow either Langmuir or Freundlich model.

The moderate polar HPD450 and polar HPD600 have several polar groups e.g. hydroxyl groups and carbonyl groups on the surfaces which are more heterogeneous than that of HPD100. Thus, the homogeneity of the surface may contribute to the variation in adsorption process.

The parameter K_F related to the adsorption capacity increased with an increase in temperature. This was in agreement with the experimental observation. Table 4.4 also exhibited that n was greater than unity, showing that saikosaponins were adsorbed favorably by the resins at the designated temperatures studied.

4.2.7 Thermodynamic of adsorption

The temperature dependence of adsorption is associated with various thermodynamic parameters. To study the thermodynamics of adsorption, experiments were carried out at 288K, 298K and 308 K. Referring to Fig.4.3, it was found that the adsorption capacity increased from 18.05 to 22.87 mg/g resin with temperature increased from 288K to 308K for an initial concentration of 26.17 mg/100ml.

Chemical thermodynamic is used to predict whether a reaction has a spontaneous tendency to occur. The thermodynamic criterion for spontaneous change at constant temperature and pressure is Gibbs energy change $\Delta G < 0$.

The apparent driving force of spontaneous change is the tendency of energy and matter to become disordered. The measure of the disorder of matter and energy used in thermodynamic is called the entropy, S . When matter and energy become

disordered, the entropy S increases (Peter Atkins 2001).

Thermodynamic parameters such as Gibbs energy change (ΔG), enthalpy change (ΔH) and entropy change (ΔS) for the adsorption of saikosaponins on adsorbent resins are summarized in Table 4.5.

The Gibbs energy change was evaluated by

$$\Delta G = - RT \ln K_L \quad (9)$$

where K_L is the adsorption equilibrium constant in the Langmuir model, T is the absolute temperature (K) and R is the universal gas constant (8.314J/mol K).

Equation (9) shows that $K_L > 1$ if $\Delta G < 0$. In general, $K_L > 1$ implies that products are dominant at equilibrium. Thus a reaction is thermodynamically feasible if $\Delta G < 0$. Conversely, $K_L < 1$ if $\Delta G > 0$. Thus a reaction with $\Delta G > 0$ is not thermodynamically feasible.

ΔH and ΔS were determined from the Van't Hoff equation (10)

$$\ln K_L = \frac{\Delta S}{R} - \frac{\Delta H}{RT} \quad (10)$$

ΔH and ΔS were obtained from the slope and intercept of the plot of $\ln K_L$ vs $1/T$ as shown in Fig.4.15.

Table 4.5 Thermodynamic parameters for the adsorption process of saikosaponins on three resins

Absorbent	ΔH (kJ/mol)	ΔG (kJ/mol)			ΔS (kJ/mol K)
		288 K	298 K	308 K	
HPD100	38.62	-29.55	-31.39	-34.29	0.24
HPD450	39.24	-27.81	-30.19	-32.47	0.23
HPD600	68.65	-26.84	-30.14	-33.47	0.33

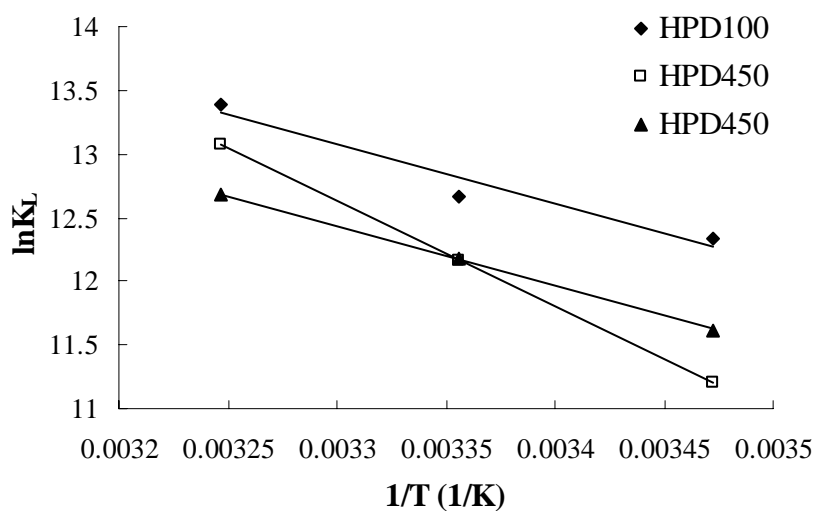


Figure 4.15 The Van't Hoff plot

In general, the Gibbs energy change ΔG for physical adsorption is smaller than that of chemisorption. The former is in the range of zero to -20 kJ/mol and the latter is in the range of -80 to -400 kJ/mol. In this study, the values of ΔG for the three resins at different temperatures were in the range between those of physical adsorption and chemisorption. It indicated that the adsorption of saikosaponins molecules on three resins is a physical adsorption enhanced by the electrostatic effect. For physical adsorption, the adsorbates are held on the surface of adsorbents by weak van der Waals forces. The polarization of adsorbates may occur but no electron transfer. For chemisorption, the adsorption occurred by involving a formation of a chemical bond between the adsorbates and the surface of the adsorbents. The formation of chemical bond is by electron transfer.

The negative value of ΔG shows the adsorption of saikosaponins on the resins is spontaneous in nature. The more negative values of ΔG imply a greater driving force to the adsorption process. As the temperature increases, the ΔG values become more negative, indicating more driving force and thus resulting in higher adsorption capacity at higher temperatures.

The values of ΔH are positive, indicating that the adsorption process is endothermic in nature. The positive value of ΔS shows the increased randomness at the

solid/solution interface during the adsorption process. In aqueous solution, the nonpolar and hydrophobic saikosaponins molecules are bound around by water molecules. When the saikosaponins molecules are adsorbed on the surface of a solid, the ordered water structure is disrupted and increases the disorder of the system. Thus the change in entropy is positive (Frank L. Slejko 1985).

4.2.8 Adsorption kinetics

In order to investigate the saikosaponins adsorbed as a function of time for HPD100, HPD450 and HPD600 resins, static experiments were carried out to evaluate the adsorption rate of saikosaponins in the condition at $\text{pH } 5.0 \pm 0.1$, $298.0 \pm 0.5 \text{ K}$, $1.00 \pm 0.01 \text{ g adsorbents}$ and initial saikosaponins concentration of $22.70 \pm 0.17 \text{ mg/100ml}$.

Fig.4.16 illustrates the extent of saikosaponins adsorbed with time on HPD100, HPD450 and HPD600 resins. The extent of saikosaponins adsorbed on HPD100 within the first hour (initial steep slope) is more significant than that on HPD450 and HPD600 resins. The difference in adsorption rate may be attributed to their different pore structures. Referring to Fig.4.1, the mesopore region ($D > 10 \text{ nm} \ \& \ D < 50 \text{ nm}$) of HPD100 resin is more dominant than those of HPD450 and HPD600 resins. In this

region, the adsorbates, saikosaponins, experience less diffusion resistance, thus facilitating diffusion through the pores into active sites for adsorption.

In addition, the curves of HPD100 and HPD450 resins have steep slopes within the first hour and gradually become gentle. During the first hour, the adsorption of the saikosaponins molecules occurs by diffusing into active sites in the macropore and mesopore region. After the first hour, adsorption rate gradually decreases. It exhibits that the active sites in macropore and mesopore regions are used up. Then, the saikosaponins molecules gradually diffuse into the micropore region for adsorption and reaches equilibrium finally.

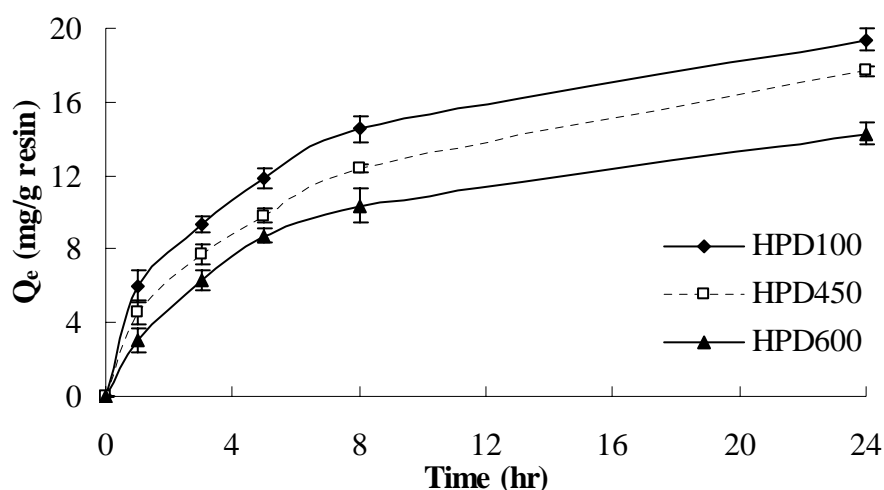


Figure 4.16 The adsorption capacities of saikosaponins on HPD100, HPD450 and HPD600 resins as a function of time (pH 5.0 ± 0.1 , 1.00 ± 0.01 g adsorbent, temperature 298.0 ± 0.5 K and agitation 150 rpm).

The kinetic adsorption data were processed and analyzed by pseudo-first order and pseudo-second order models (Kalavathy et al., 2005) in order to understand the dynamics of the adsorption process in terms of the order of the rate constant.

The pseudo first-order rate expression of Lagergren model is generally expressed as follows:

$$\frac{dQ_t}{dt} = k_1(Q_e - Q_t) \quad (11)$$

The integrated form of equation (11) is

$$\ln(Q_e - Q_t) = \ln Q_e - k_1 t \quad (12)$$

or $-\ln(1-F) = k_1 t$ where $F = \frac{Q_t}{Q_e}$

where Q_t is the adsorption capacity at the contact time (mg/g resin), k_1 is the pseudo-first order rate constant (hr^{-1}). The plots of $\ln(Q_e - Q_t)$ as a function of adsorption time are shown in Fig.4.17. The rate constants k_1 can be obtained from the slope of the linear plots.

The pseudo second-order rate equation is expressed as:

$$\frac{dQ_t}{dt} = k_2(Q_e - Q_t)^2 \quad (13)$$

The integrated form is shown as

$$\frac{t}{Q_t} = \frac{1}{k_2 Q_e^2} + \frac{t}{Q_e} \quad (14)$$

where k_2 is the pseudo-second order rate constant ($\text{g resin mg}^{-1}\text{hr}^{-1}$). The plots of $\frac{t}{Q_t}$ against t are shown in Fig.4.18. The rate constant k_2 can be obtained from the intercept of the linear plots. The adsorption rate constants and the correlation coefficients r^2 are listed in Table 4.6.

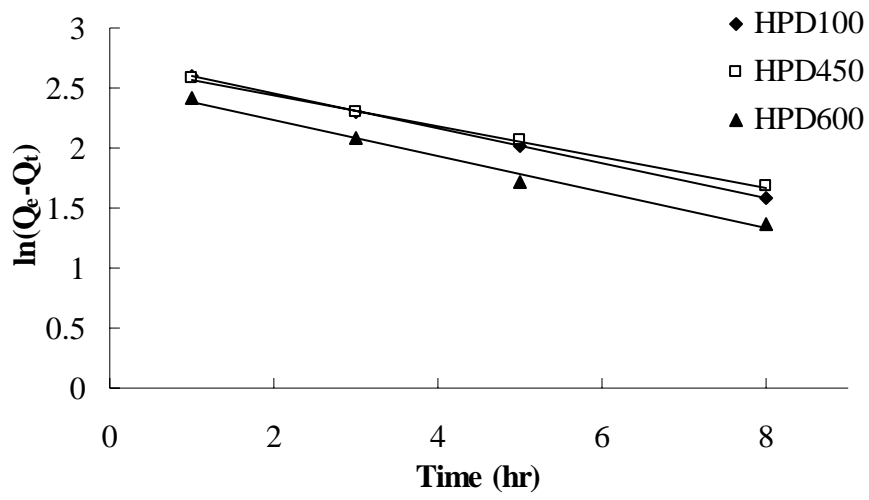


Figure 4.17 The plots of the pseudo-first order kinetics on the three resins.

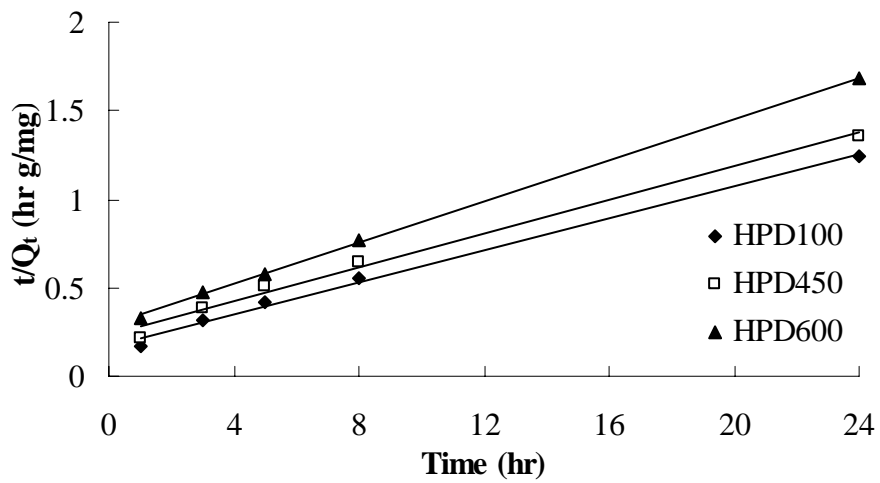


Figure 4.18 The plots of pseudo second-order kinetics on the three resins.

Table 4.6 The parameters of adsorption kinetics for saikosaponins on the three resins

Resins	First-order constants		Second-order constants	
	k_1 (1/hr)	r^2	k_2 (g resin/mg hr)	r^2
HPD100	0.14	1	0.012	0.995
HPD450	0.13	0.999	0.010	0.991
HPD600	0.15	0.989	0.012	0.999

For all resins, the r^2 obtained from the two models were further analyzed by ANOVA.

The results showed that there is no significant difference between the r^2 of the two models for all resins. Please refer to Appendix A.2 for details.

Thus it can be concluded that the adsorption of saikosaponins on HPD100, HPD450 and HPD600 resins follow either the pseudo-first order model or the pseudo-second order model.

Generally, adsorption process can be described as a series of steps (Klaus et al.,1995):

- 1) Transport of the adsorbates from bulk solution to the adsorbent exterior surface across the boundary layer(film diffusion);
- 2) Transport of the adsorbates within the porous adsorbent (intraparticle diffusion);
- 3) Adsorption of the adsorbates on the interior surface of the adsorbent.

The film diffusion and intraparticle diffusion of adsorbate is shown in Fig.4.19.

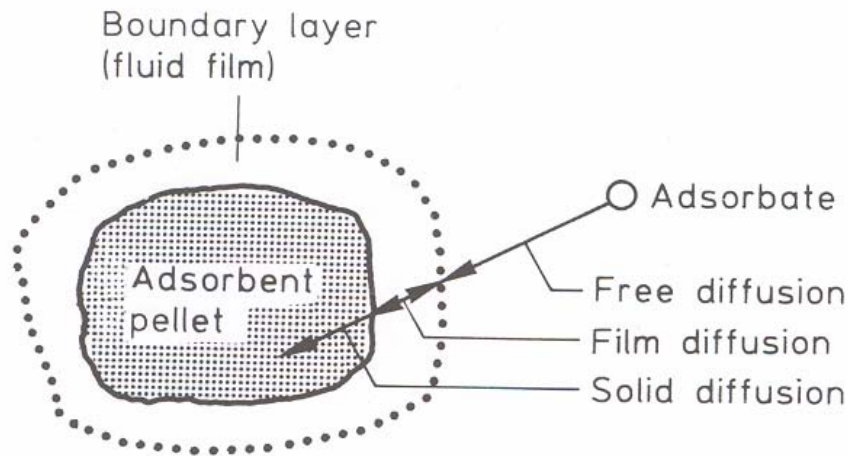


Figure 4.19 The diffusion of adsorbate (cited from Klaus et al.,1995)

To determine which step (film diffusion or intraparticle diffusion) is the rate limiting step and also find the rate parameters for film diffusion or intraparticle diffusion, the adsorption kinetic data were further processed. The two diffusion models can be presented as:

$$\text{Film diffusion model: } \ln(1-F) = - R't \quad (14)$$

$$\text{Intraparticle diffusion model: } Q_t = k_p t^{1/2} \quad (15)$$

where R' is the diffusion rate parameter for film diffusion model, k_p is the diffusion rate parameter for intraparticle diffusion model.

The value of R' can be directly obtained from the slope of the plot of $-\ln(1-F)$ against t . The value of k_p can be obtained from the slope of the plot of Q_t against $t^{1/2}$.

Table 4.7 The diffusion rate parameters

Resins	$\ln(1-F) = -R't$		$Q_t = k_p t^{1/2}$	
	R' (1/hr)	r^2	k_p (mg/g resin $t^{1/2}$)	r^2
HPD100	0.14	1	3.68	0.962
HPD450	0.13	0.999	3.32	0.980
HPD600	0.15	0.989	2.77	0.943

Referring to Table 4.7, the correlation coefficients show that the film diffusion model can give good fitting to the adsorption kinetic data of the saikosaponins adsorbed on HPD100, HPD450 and HPD600 resins. It indicated that film diffusion is the main rate limiting step for the adsorptions of saikosaponins on three types of resins.

As mentioned before, adsorption composes of a series of steps. The first two steps are mass transfer process. Mass transfer process occurs when a component in a mixture migrates in the same phase or from phase to phase because of a difference in concentration between two points. The slowest mass transfer step controls the total adsorption rate. In the liquid phase adsorption, the flow rate of carrier phase – liquid

is low. Thus, a pronounced boundary layer develops around the adsorbent particles.

The diffusion resistance of the boundary layer is large. On the contrary, the sizes of the pores are much larger than those of saikosaponins molecules. Thus, the saikosaponins molecules experience less diffusion resistance inside the particles. As a result, the diffusion resistance of the boundary layer is larger than that inside the particles and the film diffusion limits the process.

After evaluating the adsorption capacities, adsorption efficiencies and desorption efficiencies of the eight resins, HPD100 was selected as the most appropriate resin for adsorption of saikosaponins because of its highest adsorption capacity and adsorption efficiency among all the resins. Thus, it was chosen as the resin for dynamic study.

Referring to the results of thermodynamic study, it was found that the adsorption process was endothermic and spontaneous in nature, respectively. Also, the rate of adsorption process was controlled by the film diffusion.

5. Dynamic study

5.1 Experimental section

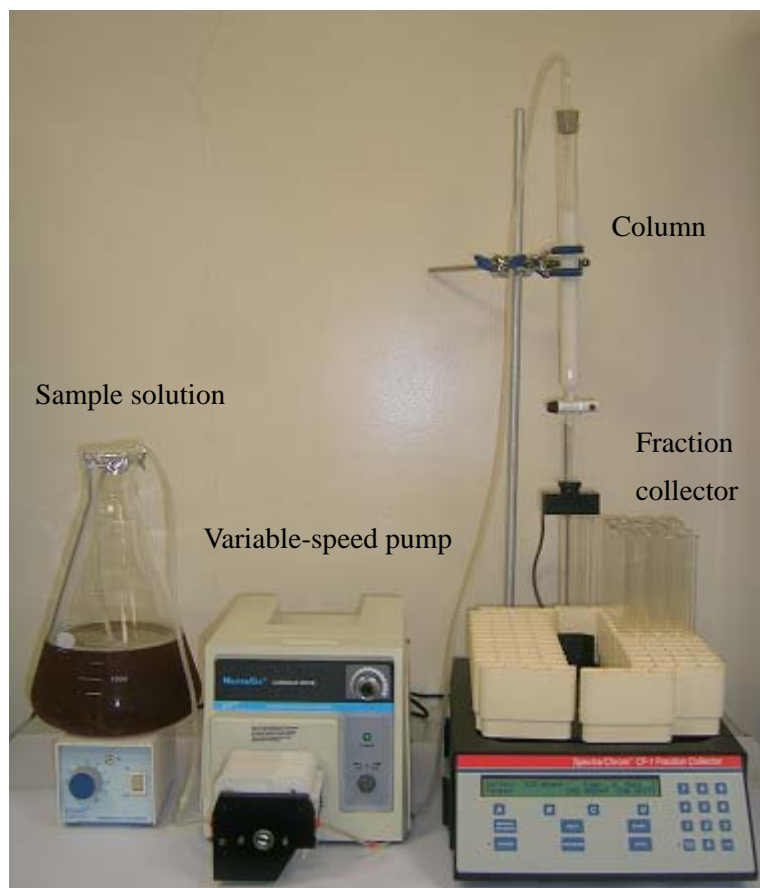
5.1.1 Adsorption separation process

A whole adsorption separation process included four successive steps in sequential: conditioning, adsorption, washing and elution in sequential. First, the column was conditioned with de-ionized water. Then, the sample solution was loaded onto the column until the end of adsorption. After that, the column was washed with a certain volume of de-ionized water in order to remove the impurities. Finally, the loaded column was eluted with a certain volume of aqueous ethanol solution of varying step-gradient from 20 to 100%.

5.1.2 Low pressure liquid chromatography (LPLC) system and column conditioning

The low pressure liquid chromatography system equipped with a Masterflex L/S variable-speed console drive pump (Cole-Parmer Instrument Company, USA) and a Spectra/Chrom® CF-1 fraction collector (Spectrum Chromatography, Houston, TX USA). The packing material, HPD100 resin was wet with the absolute ethanol to solvate its functional group before being packed in a glass column with inside diameter of 1.75 ± 0.05 cm and length of 25 cm. The packed column was then washed with distilled water to activate itself for working properly to aqueous samples. The

operating temperature was $25.0 \pm 0.5^{\circ}\text{C}$. The experimental set-up for dynamic adsorption is shown in Picture 5.1.



Picture 5.1 The experimental set-up for dynamic adsorption.

5.1.3 Dynamic adsorption

The sample solution with known concentration of saikosaponins (sum of concentration of saikosaponin a and saikosaponin c) was fed to the top of the glass column at a certain feed flow rate regulated by the variable-speed pump. The effluents collected at intervals by the fraction collector were monitored by HPLC for

compositional analysis. The operating parameters including the feed flow rate, the feed concentration (C_{in}) of saikosaponins and the bed depth (BD) were varied to investigate their effects on the breakthrough point of the breakthrough curve. The breakthrough point was indicated when the relative concentration of saikosaponins C_{exit}/C_{in} of the effluent reached 0.05, where C_{exit} is the exit concentration. The experimental conditions are listed in Table 5.1.

Table 5.1 The experimental conditions for column tests

Experimental conditions	Run 1			Run 2		Run 3	
Feed flow rate (m/min)	1	2	3	2	2	2	2
Feed concentration (mg/ml)	0.193	0.180	0.191	0.101	0.304	0.322	0.325
Bed depth (cm)	12	12	12	12	12	16	20

5.1.4 Dynamic desorption

The loaded column was first washed with de-ionized water and then desorbed with aqueous ethanol solution of varying step-gradient from 20 to 100%. The effluent fractions collected at intervals were monitored by HPLC for compositional analysis. Each effluent fraction was concentrated, dried in oven and weighed for further analysis.

5.1.5 Evaluation of the column performance

The effluent fractions for each step in the adsorption separation process were collected for compositional analysis. Based on the compositions of saikosaponins in all the effluent fractions, the adsorption and desorption performance of the column could be evaluated.

For the adsorption, the dynamic adsorption curves (breakthrough curves) of saikosaponins were established to investigate the effects of the variable condition parameters on the breakthrough point and to evaluate the suitable loading volume for the adsorption step.

For the desorption, the dynamic elution curves of saikosaponins were established to find the appropriate step-gradient elution program for achieving an efficient separation in the elution step.

The column performance indices for desorption including purity, concentration ratio and yield of saikosaponins are defined as follows:

Purity = fractional mass of saikosaponins in the concentrated effluent fraction

$$\text{Concentration ratio} = \frac{\text{purity of saikosaponins in the concentrated effluent fraction}}{\text{purity of saikosaponins in the sample solution}}$$

$$\text{Yield} = \frac{\text{mass of saikosaponins in the concentrated effluent fraction}}{\text{sum of masses of saikosaponins in the sample solution}}$$

5.2 Results and discussion

5.2.1 Dynamic adsorption

The dynamic adsorption experiments were carried out on the packed column at a certain feed flow rate, feed concentration and bed depth. For each experiment, the effluent fractions of the adsorption step were collected in several intervals, e.g. 15-18 ml for each interval, for compositional analysis. To avoid the loss of saikosaponins from the adsorption stage, the breakthrough point of the breakthrough curve was set at the point as the exit concentration (C_{exit}) of saikosaponins approached 5% of the feed concentration. The loading volume of the adsorption stage was then selected according to the elution volume at the breakthrough point. The breakthrough curves of saikosaponins with the variable feed flow rate, feed concentration and bed depth, respectively, are shown in Fig.5.1-5.3 and discussed next.

5.2.1.1 Effect of feed flow rate

It can be seen from Fig. 5.1 that the breakthrough point was reached earlier as the feed flow rate increased. The earlier breakthrough at high flow rate may be attributed to the effect of feed flow rate on the intraparticle diffusion of saikosaponins molecules into the interior surface of the resins for adsorption. Since the feed flow rate was too fast, the residence time for the saikosaponins molecules in the resin was decreased.

Therefore, the time for interaction between the resin and the saikosaponins molecules was decreased. The saikosaponins molecules did not have enough time for diffusion through the pores into the interior active sites for adsorption, thus the leakage occurred earlier. As a result, the amount adsorbed decreased when the feed flow rate increased.

Table 5.2 shows the breakthrough volume (BV), breakthrough time (BT) and amount of adsorbed (AA) at the breakthrough points in three feed flow rates.

Table 5.2 The BV, BT and AA at the breakthrough points in three feed flow rates.

Feed flow rate (ml/min)	C _{in} (mg/ml)	BV (ml)	BT (min)	AA (mg)
1	0.193 ± 0.008	639.0 ± 2.0	639.0 ± 2.0	123.33 ± 4.73
2	0.180 ± 0.009	206.0 ± 4.0	103.0 ± 2.0	37.08 ± 1.13
3	0.191 ± 0.007	69.0 ± 5.0	23.0 ± 1.7	13.18 ± 0.47

Based on the findings from Table 5.2, the feed flow rate of 2 ml/min was selected in order to have an efficient column operation to balance the loading amount of saikosaponins and the operating time, will then be used in further study.

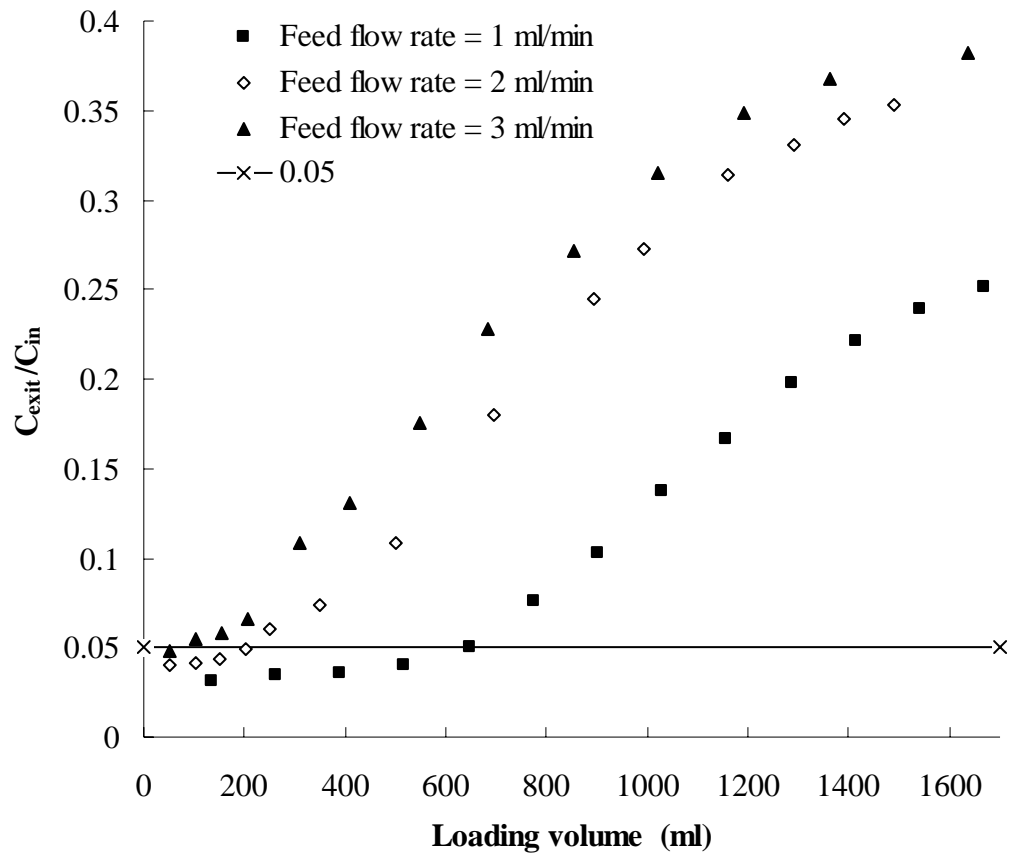


Figure 5.1 The breakthrough curves of saikosaponins adsorption in various three feed flow rates. ($T = 25.0 \pm 0.5^\circ\text{C}$, $C_{in} = 0.188 \pm 0.007 \text{ mg/ml}$ and $BD = 12\text{cm}$)

5.2.1.2 Effect of feed concentration

Fig. 5.2 shows the breakthrough occurred earlier as the feed concentration increased.

The phenomenon exhibited that the time for breakthrough point decreased as the feed concentration increased. Table 5.3 shows the BV, BT and AA at the breakthrough points in three feed concentrations.

Table 5.3 The BV, BT and A A at the breakthrough points in three feed concentrations.

Feed flow rate (ml/min)	C _{in} (mg/ml)	BV (ml)	BT (min)	AA (mg)
2	0.101 ± 0.005	625.0 ± 4.0	312.5 ± 2.0	63.13 ± 2.72
2	0.180 ± 0.009	206.0 ± 4.0	103.0 ± 2.0	37.08 ± 1.13
2	0.304 ± 0.01	156.0 ± 5.0	78.0 ± 2.5	47.42 ± 0.05

Based on Table 5.3, the feed concentration of 0.304 mg/ml was selected in order to balance the loading amount of saikosaponins and the operating time. This feed concentration will be used in further study.

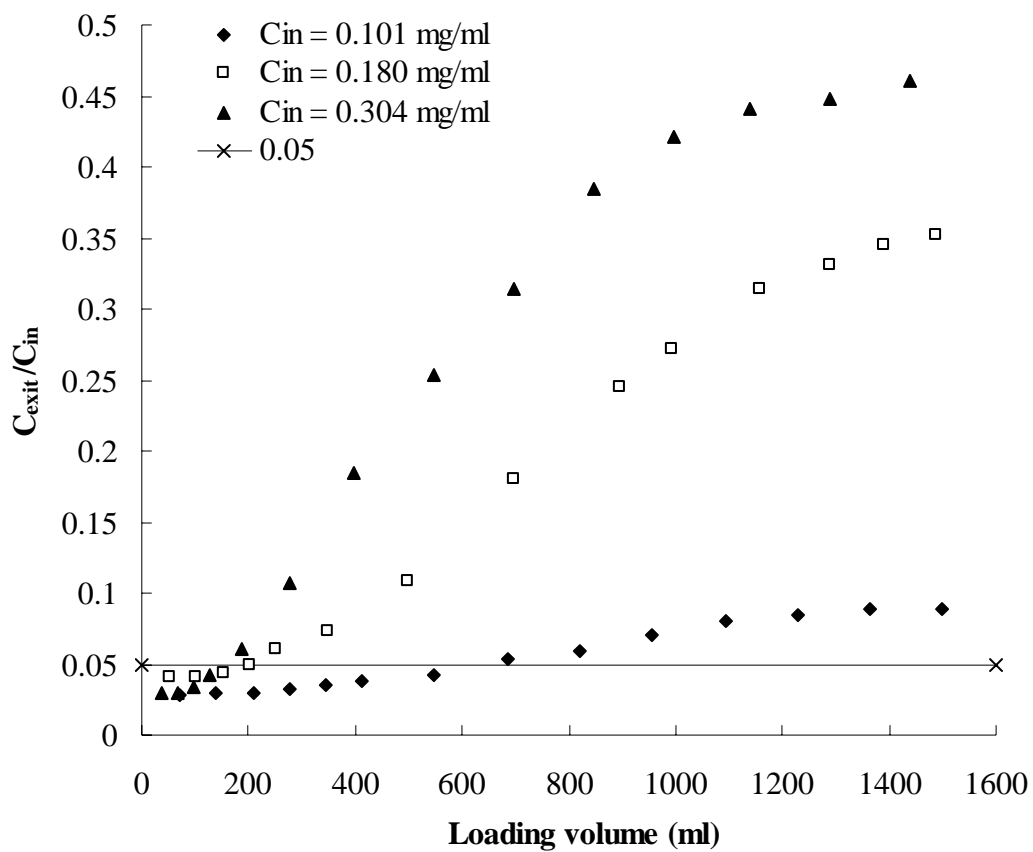


Figure 5.2 The breakthrough curves of saikosaponins adsorption in various feed concentrations. ($T = 25.0 \pm 0.5^\circ\text{C}$, feed flow rate = 2 ml/min and BD = 12cm)

5.2.1.3 Effect of bed depth

As shown in Fig.5.3, the breakthrough point took place earlier as the bed depth decreased. It indicated that the time for breakthrough point is roughly proportional to the bed depth at a given feed flow rate and feed concentration. Since the amount of resin packed in the column increased with the bed depth, the amount of saikosaponins adsorbed up to the breakthrough point increased. Thus, the leakage occurred later.

Table 5.4 shows the BV, BT and A A at the breakthrough points in three bed depths.

Table 5.4 The BV, BT and A A at the breakthrough points in three bed depths.

Bed depth (cm)	BV (ml)	BT (min)	AA (mg)
12	156.0 ± 5.0	78.0 ± 2.5	47.42 ± 0.05
16	279 ± 6.0	139.5 ± 3.0	89.84 ± 1.42
20	426 ± 4.0	213 ± 2.0	138.45 ± 2.96

Referring to Table 5.4, the bed depth of 20 cm was selected for further study. As this set up could achieve higher loading amount of saikosaponins in an appropriate operating time. If the operating time is short, the number of times for regenerating the column will increase and thus increase the energy cost in column regeneration.

Based on the findings in Table 5.2-5.4, the conditions for an efficient column

operation in terms of the loading amount and the operating time could be found out.

For HDP100 resin, the feed flow rate of 2 ml/min was selected and the loading volume was around 400 to 450 ml at the C_{in} of 0.300 to 0.340 mg/ml. This experimental set up will be applied in the desorption step.

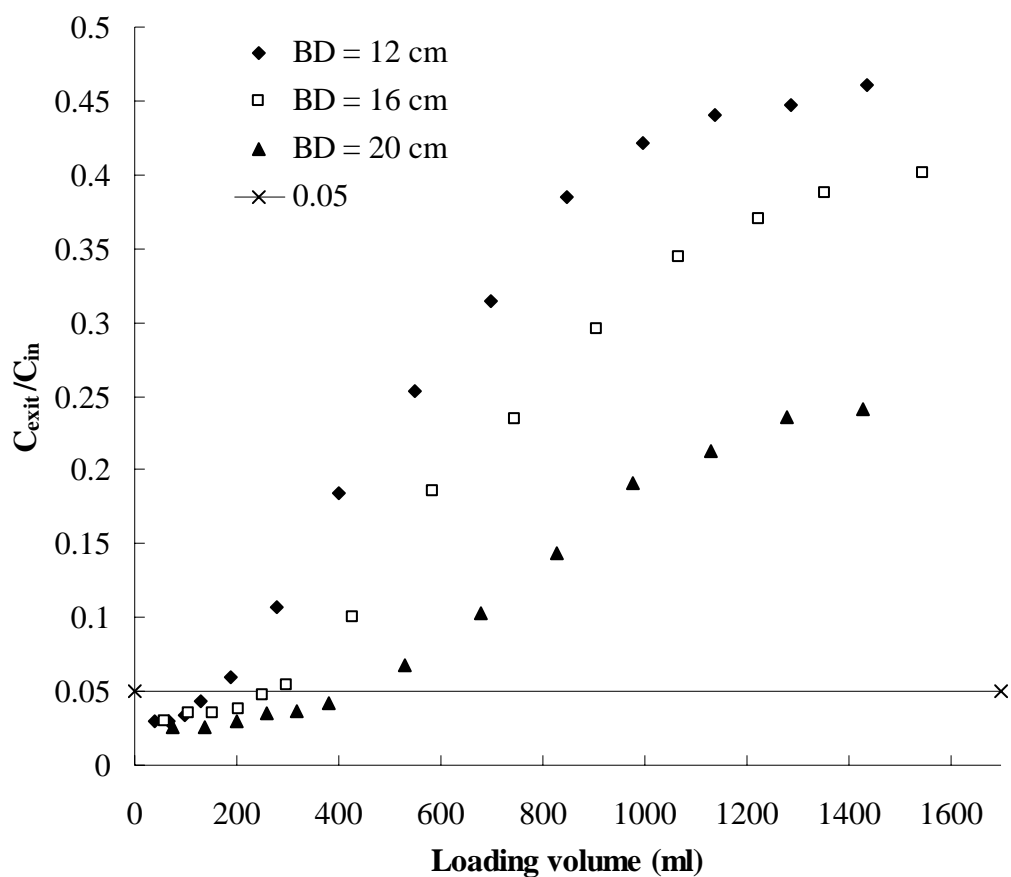


Figure 5.3 The breakthrough curves of saikosaponins adsorption in various bed depths. ($T = 25.0 \pm 0.5^{\circ}\text{C}$, feed flow rate = 2 ml/min and $C_{in} = 0.317 \pm 0.011$ mg/ml)

5.2.1.4 Concentration profiles of saikosaponins in the fixed-bed

In the fixed-bed adsorption, the concentrations of saikosaponins (adsorbate) in the sample solution (liquid phase) and the resin (solid phase) change with time and position in the bed when adsorption proceeds.

At the start of the process, the resin at the inlet of the bed contains no saikosaponins.

As the sample solution first contacts the resin at the inlet of the bed, mass transfer occurs due to the concentration gradient and adsorption takes place there.

When the sample solution passes through the bed, the concentration of saikosaponins in the sample solution decreases very rapidly with distance in the bed to zero before the end of the bed is reached. This concentration profile is shown by curve t_1 in Fig.5.4, where the relative concentration C/C_{in} is plotted against the bed length. C_{in} refers to the feed concentration and C refers to the saikosaponins concentration at a point in the bed. After a short time, the resin near the inlet is nearly saturated, and most of mass transfer or adsorption takes place farther from the inlet, as shown by curve t_2 . After a period of time, the profile or mass-transfer zone where most of the change in concentration occurs has moved farther down along the bed, as shown by curves t_3 and t_4 .

The concentration profiles shown are for the liquid phase. Similar profiles could be drawn for the average concentration of adsorbate on the resin, showing nearly saturated resin at the inlet, a large change in the region of the mass-transfer zone and zero concentration at the end of the bed.

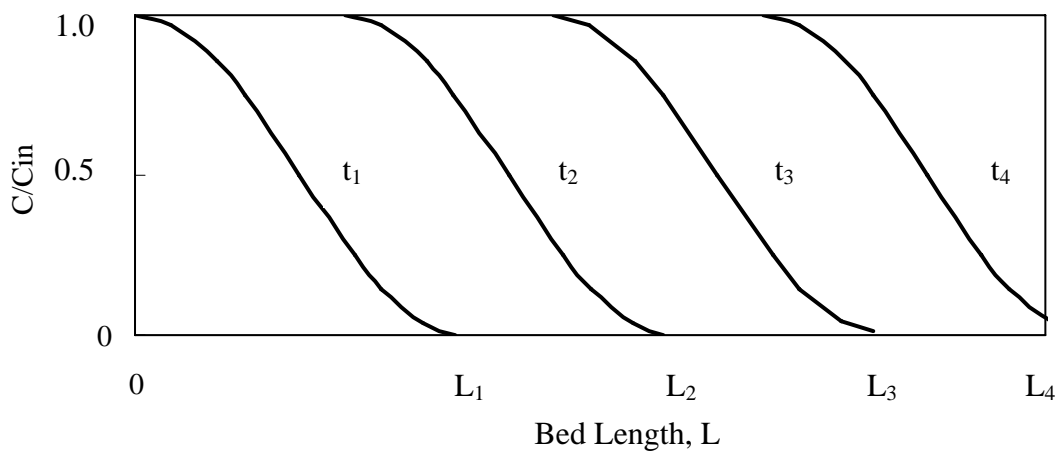


Figure 5.4 The concentration profiles for adsorption in a fixed bed. (cited from Warren et al.,2005)

5.2.1.5 Breakthrough curve

As shown in Fig.5.4, the major part of the adsorption at any time takes place in a relatively narrow mass transfer zone. As the sample solution continues to flow through, this mass transfer zone, which is S-shaped, moves down along the column.

At time t_1 and t_2 , the outlet concentration is approximately zero, as shown in Fig.5.5.

This outlet concentration remains nearly zero until the mass-transfer zone starts to

reach the outlet of the bed at time t_3 . Then the outlet concentration starts to rise. At time t_4 , when the outlet concentration reaches a limiting value or breakthrough point, the loading of the sample solution is stopped or diverted to a fresh adsorbent bed. The breakthrough point is commonly taken as 0.05 to 0.1 for the relative concentration of $C_{\text{exit}}/C_{\text{in}}$. Since this concentration occurred only in the last portion of the sample solution fed, the average fraction of adsorbate adsorbed from the start to the breakthrough point is often 0.95 or higher.

After the breakthrough point is reached, the exit concentration rises rapidly until the bed is considered as ineffective when the end of the breakthrough curve is.

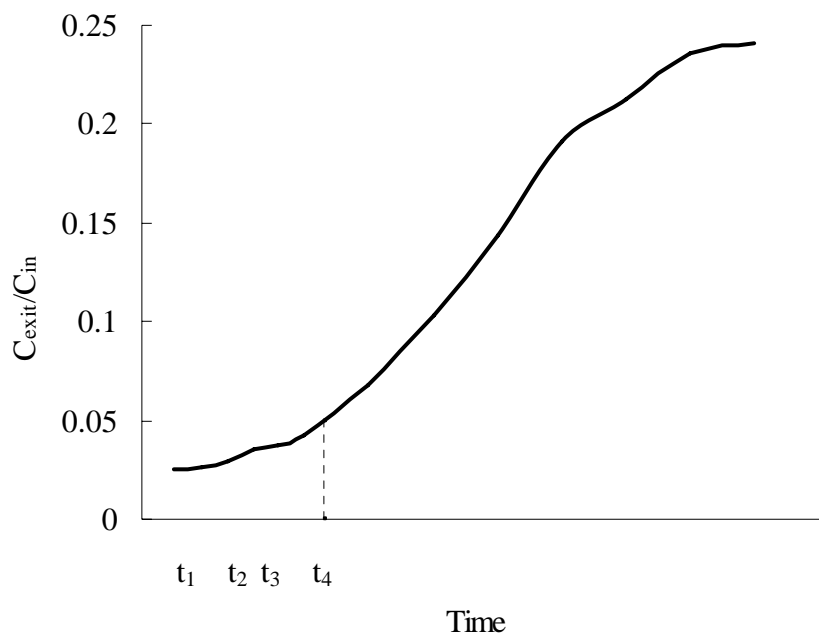


Figure 5.5 The Breakthrough curve for adsorption in the fixed bed.

5.2.2 Dynamic desorption

The dynamic desorption experiments were carried out after loading the sample solution with a suitable loading volume and a desired feed concentration found in the adsorption step. The loaded column was first eluted with 120-200 ml of de-ionized water followed by a certain volume of aqueous ethanol solution of varying step-gradient from 20 to 100% at a flow rate of 2 ml/min. The effluent fractions of the elution step were collected in several intervals, e.g. 40 ml for each interval, for compositional analysis.

The experiments were conducted in different step-gradient elution program of aqueous ethanol solution in order to investigate their effects on the elution performance of the column.

5.2.2.1 Elution solvent

The relation among the adsorbate, the adsorbent and the eluent is formed based on the “like attracts like” principle. The relative strength of attraction between them determines whether the adsorbate will stay in the adsorbent or in the eluent.

In this study, the hydrophobic HPD100 resin adsorbs hydrophobic saikosaponins

molecules from aqueous solution because they are alike. The attraction between them is van der Waals forces.

The adsorbate could be eluted from the resin if the attraction between the adsorbate and the eluent is greater than that between the adsorbate and the resin. Thus an appropriate solvent is chosen to disrupt the van der Waals forces that retain the adsorbate.

The aqueous ethanol is chosen as the only elution solvent in the study because saponins have high solubility in ethanol. Thus, mostly adsorbed saponins could be desorbed from the resin. In addition, ethanol is non-toxic and environmental friendly. Since the concentrated and purified saikosaponins molecules desorbed from the resin is recovered for use in medicinal supplementary food. Therefore, the non-toxic property of the solvent is very important.

In this study, gradient elution is employed rather than isocratic elution as the former could enhance the separation efficiency. Here two solvents system (water and ethanol) that differs in polarity is employed. During the elution process, the ratio of the solvents is varied in a series of steps with time. The polarity of elution solvents is

changed from polar to non-polar with time in this study. If the relatively polar impurities match with the polarity of solvent, they will be eluted out first. Then, the relatively non-polar saikosaponins molecules will be eluted out later. As a result, the saikosaponins molecules can be separated from the impurities and an efficient separation is achieved.

5.2.2.2 Dynamic elution curve

Four step-gradient elution programs were designed to investigate their effects on the desorption performance of the column. The details are shown in Table 5.5.

Table 5.5 Four step-gradient elution programs

Programs	Step-gradient elution (in % ethanol)
1	200ml (0%), 200ml (30%), 200ml (60%) and 120ml (90%)
2	160ml (0%), 120ml (30%), 120ml (50%), 200ml (60%) and 120ml (90%)
3	120ml (0%), 120ml (20%), 120ml (40%), 120ml (60%), 120 ml (80%) and 120ml (100%)
4	120ml (0%), 160ml (25%), 160ml (45%), 160ml (65%) and 120ml (85%)

Fig.5.6 shows the dynamic elution curves for the step-gradient elution program (1). There are three parts in the figure: the purity of saikosaponins, the mass of saikosaponins and the total mass of effluent against the elution volume are shown in parts (a)-(c) respectively. The results of part (b) show that the majority of saikosaponins were eluted by 60% ethanol. It showed that a higher percentage of ethanol was favorable for the desorption of saikosaponins. The results of part (b) and (c) showed that majority of impurities eluted by 0-30% ethanol were separated with the majority of saikosaponins eluted by 60% ethanol. However, it was also observed that a significant amount of impurities were eluted together with the majority of saikosaponins by 60% ethanol. As a result, the saikosaponins were not efficiently separated. Table 5.6 shows that the purity of saikosaponins in the fractions collected at 60% ethanol was only around 11%. Therefore, the step-gradient elution program (1) is needed to modify to enhance the purity.

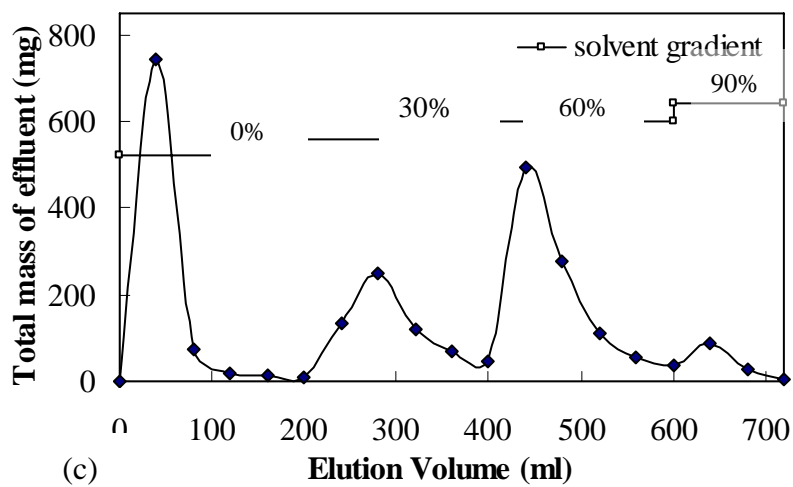
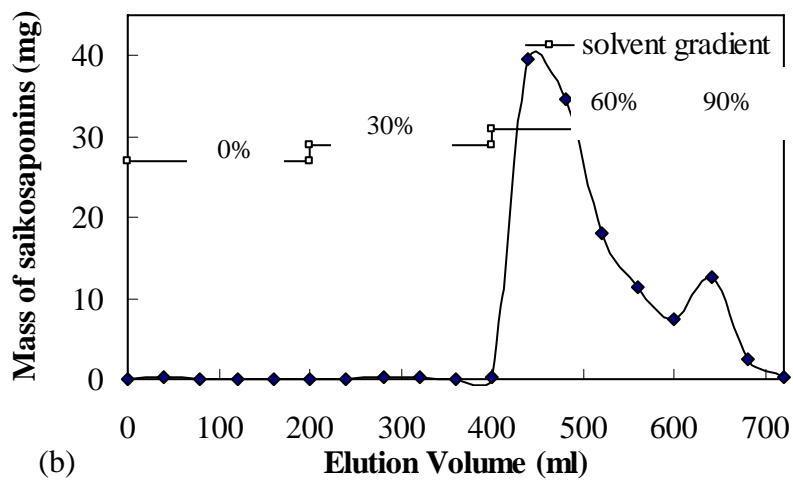
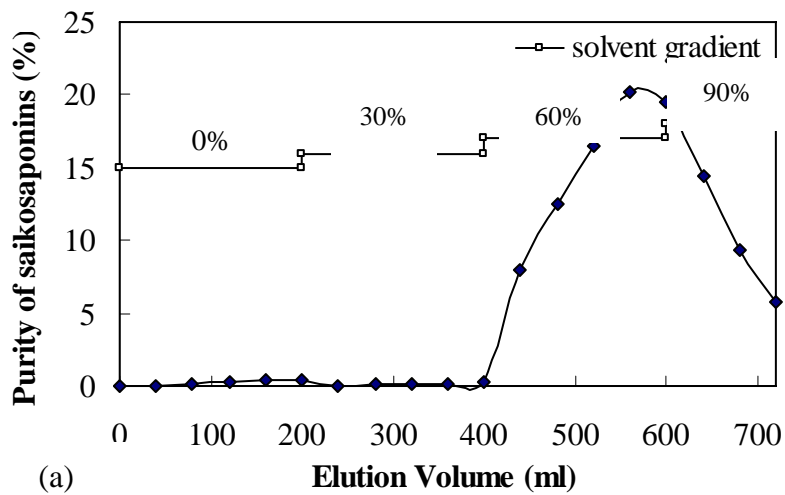


Figure 5.6 The dynamic elution curves for step-gradient elution program (1): (a) purity of saikosaponins, (b) mass of saikosaponins and (c) Total mass of effluent.

Table 5.6 Column performances of the step-gradient elution program (1)

Step of column operation	Operating volume (ml)	Effluent	Saikosaponins		
		Mass (mg)	Mass (mg)	Purity (%) ^b	Recovery yield (%) ^c
Adsorption ^a	415	9897.75	132.39	1.29	100
Step-gradient elution					
0% ethanol	200	855.60	0.43	0.05	0.33
30% ethanol	200	618.99	0.60	0.10	0.46
60% ethanol	200	973.40	110.97	11.40	83.82
90% ethanol	120	118.50	15.33	12.93	11.58
Total	/	2566.49	127.03	/	95.95
Concentration ratio				9:1	

^a Feed solution: Loading volume = 415 ml ; concentration of concentrate = 23.85 mg/ml ; concentration of saikosaponins = 0.319 mg/ml.

$$^b \text{ Purity of saikosaponins (\%)} = \frac{\text{fractional mass of saikosaponins}}{\text{fractional dry mass of effluent}} \times 100\%$$

$$^c \text{ Recovery yield (\%)} = \frac{\text{fractional mass of saikosaponins}}{\text{total loading mass of saikosaponins}} \times 100\%$$

5.2.2.3 Comparison of the column performance

The dynamic elution curves of Fig. 5.6 were then referred and the step-gradient elution program was modified in order to enhance the separation efficiency. Figs.5.7 – 5.9 show the dynamic elution curves for step-gradient program (2), (3) and (4) respectively. There are three parts in each figure as mentioned before. The column performances, in terms of purity, concentration ratio and recovery yield of saikosaponins among the four step-gradient elution programs were compared. Tables 5.7 – 5.9 show the column performances indices for step-gradient elution program (2), (3) and (4) respectively.

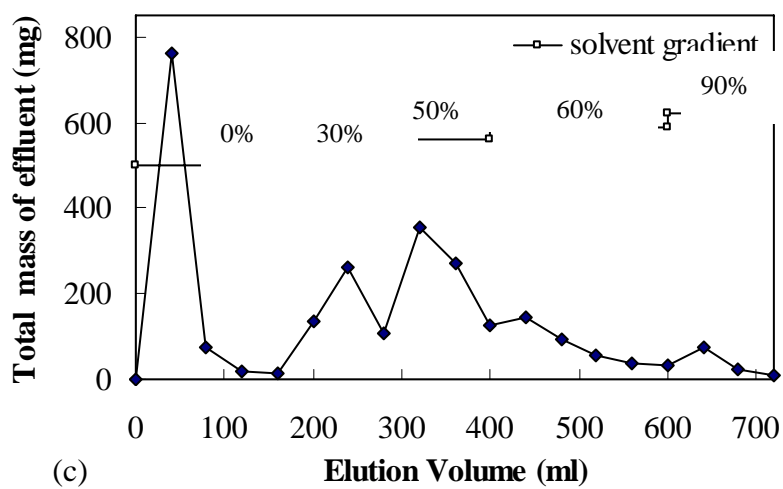
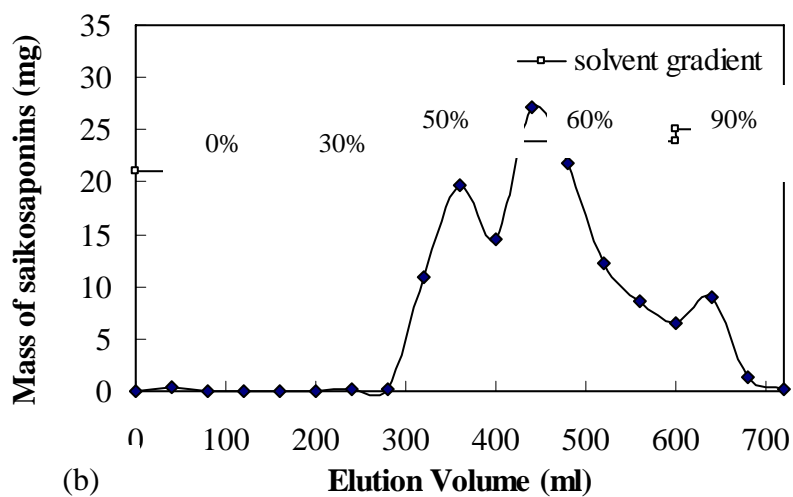
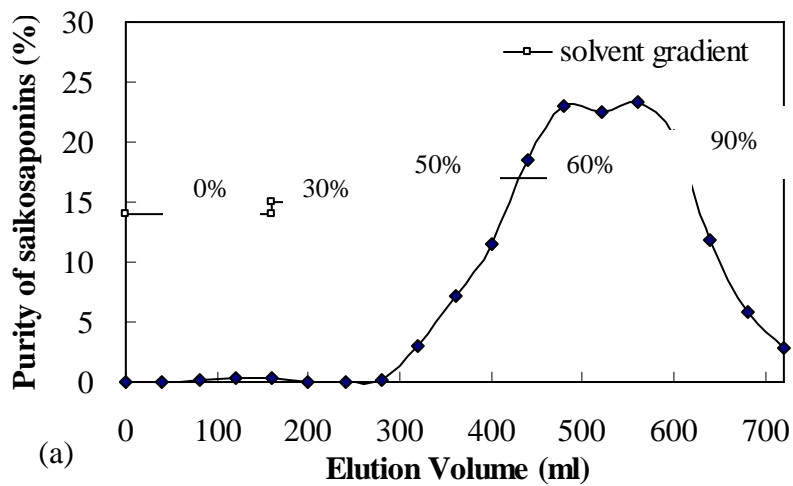


Figure 5.7 The dynamic elution curves for the step-gradient elution program (2): (a) purity of saikosaponins, (b) mass of saikosaponins and (c) Total mass of effluent .

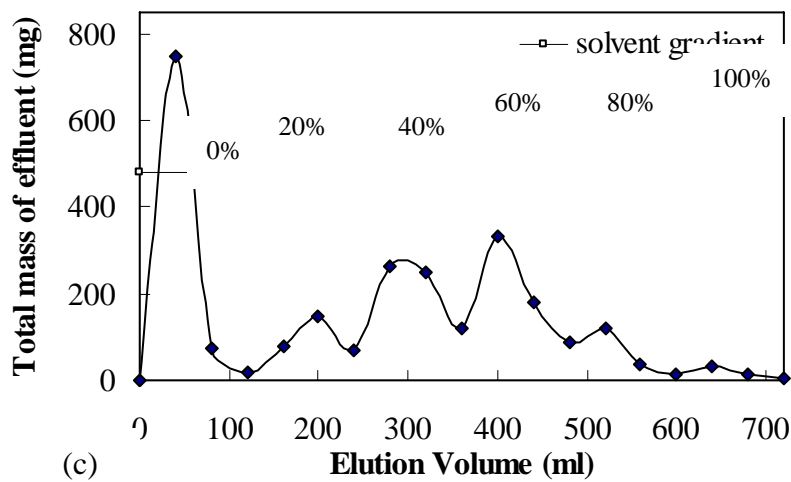
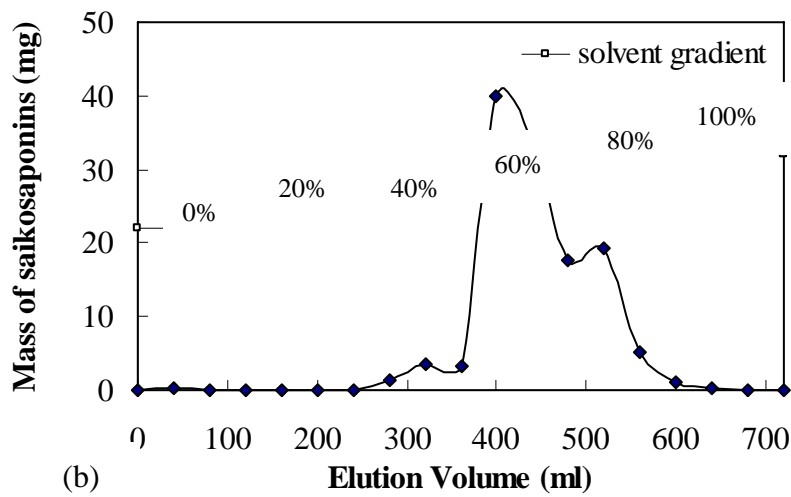
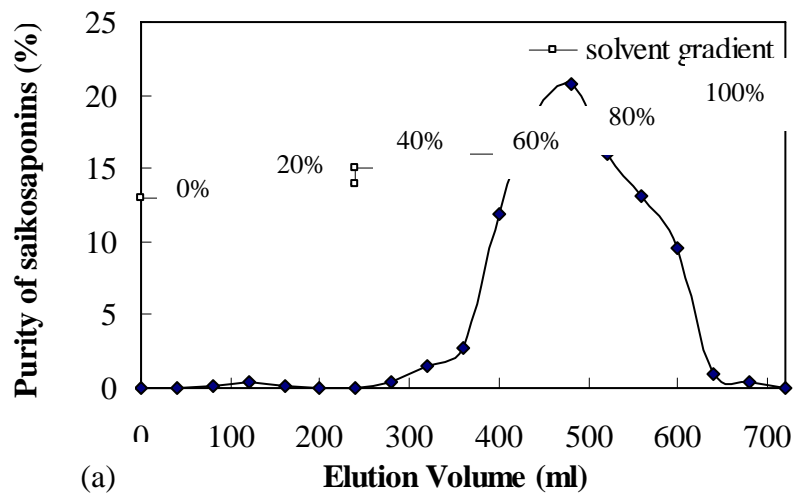


Figure 5.8 The dynamic elution curves for the step-gradient elution program (3): (a) purity of saikosaponins, (b) mass of saikosaponins and (c) Total mass of effluent.

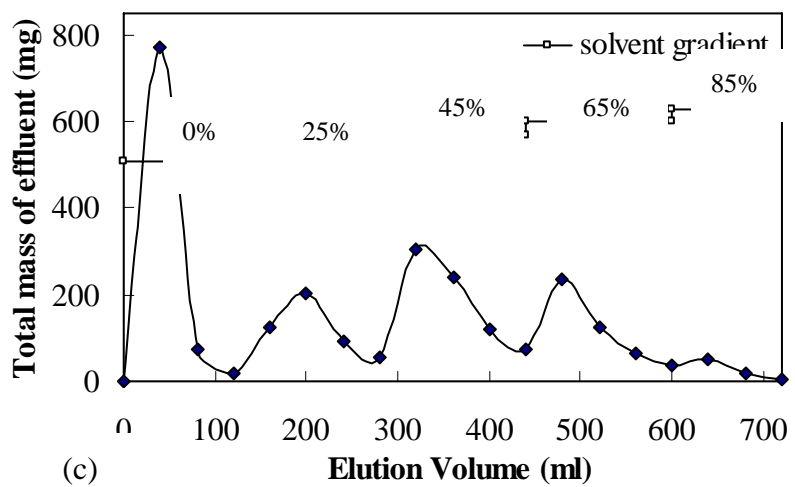
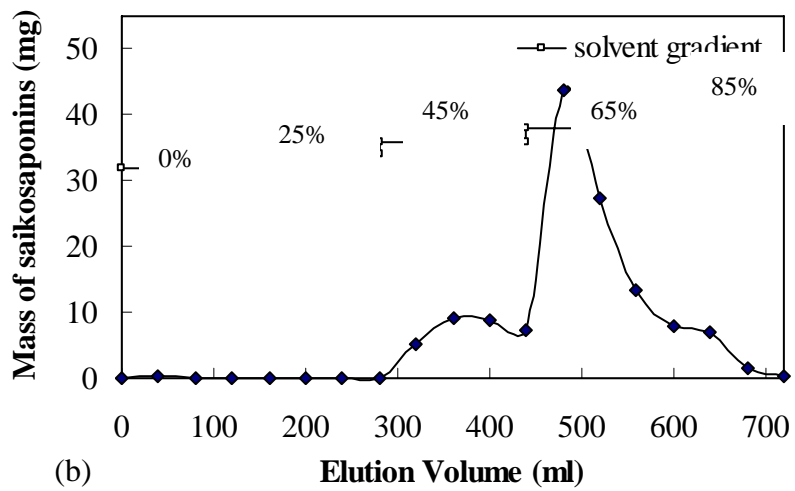
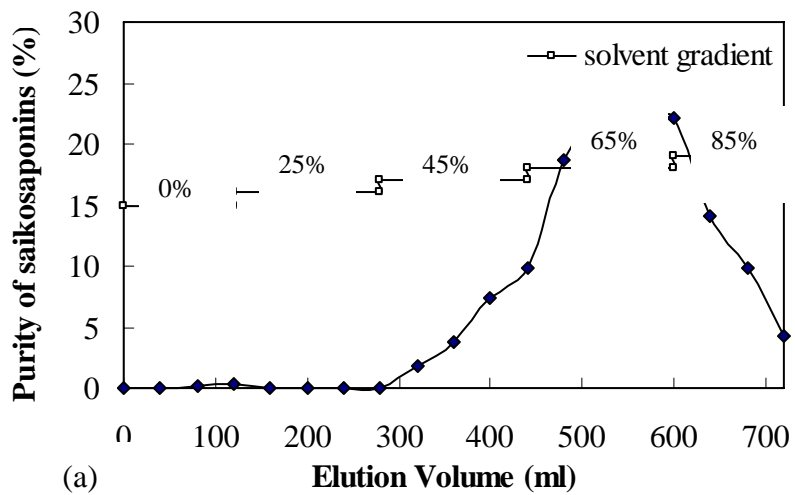


Figure 5.9 The dynamic elution curves for the step-gradient elution program (4): (a) purity of saikosaponins, (b) mass of saikosaponins and (c) Total mass of effluent

Table 5.7 Column performances of the step-gradient elution program (2)

Step of column operation	Operating volume (ml)	Effluent	Saikosaponins		
		Mass (mg)	Mass (mg)	Purity (%)	Recovery yield (%)
Adsorption ^a	415	10748.50	138.20	1.26	100
Step-gradient elution					
0% ethanol	160	869.40	0.51	0.06	0.37
30% ethanol	120	503.40	0.37	0.07	0.27
50% ethanol	120	755.20	45.09	5.97	32.63
60% ethanol	200	366.00	76.45	20.89	55.31
90% ethanol	120	106.40	10.49	9.86	7.59
Total	/	2600.40	132.68	/	96.01
Concentration ratio				17:1	

^a Feed solution: Loading volume = 415 ml ; concentration of concentrate = 25.90 mg/ml ; concentration of saikosaponins = 0.333 mg/ml.

Table 5.8 Column performances of the step-gradient elution program (3)

Step of column operation	Operating volume (ml)	Effluent	Saikosaponins		
		Mass (mg)	Mass (mg)	Purity (%)	Recovery yield (%)
Adsorption ^a	415	10904.13	138.61	1.27	100
Step-gradient elution					
0% ethanol	120	842.00	0.52	0.06	0.37
20% ethanol	120	293.40	0.18	0.06	0.13
40% ethanol	120	631.20	8.07	1.28	5.82
60% ethanol	120	600.60	91.52	15.24	66.02
80% ethanol	120	172.40	25.63	14.87	18.49
100% ethanol	120	55.70	0.41	0.73	0.29
Total	/	2595.29	126.32	/	91.13
Concentration ratio				12:1	

^a Feed solution: Loading volume = 415 ml ; concentration of concentrate = 26.28 mg/ml ; concentration of saikosaponins = 0.334 mg/ml.

Table 5.9 Column performances for the step-gradient elution program (4)

Step of column operation	Operating volume (ml)	Effluent	Saikosaponins		
		Mass (mg)	Mass (mg)	Purity (%)	Recovery yield (%)
Adsorption ^a	415	11360.63	134.46	1.16	100
Step-gradient elution					
0% ethanol	120	865.00	0.47	0.05	0.35
25% ethanol	160	478.00	0.22	0.05	0.17
45% ethanol	160	742.80	30.78	4.14	22.89
65% ethanol	160	457.60	92.47	20.21	68.77
85% ethanol	120	69.80	8.70	12.47	6.47
Total	/	2613.20	132.44	/	98.50
Concentration ratio				17:1	

^a Feed solution: Loading volume = 415 ml ; concentration of concentrate = 27.38 mg/ml ; concentration of saikosaponins = 0.324 mg/ml.

Referring to Fig. 5.6(b), it is observed that 0-30% ethanol is not capable for eluting saikosaponins but is capable for eluting majority of impurities. It is found that majority of saikosaponins, over 80%, were eluted in the fractions collected at 60% ethanol. The results indicated that the polarity of saikosaponins was matched with that of 60% ethanol and thus desorption occurred. It is also observed that a significant amount of impurities were eluted together with the majority of saikosaponins by 60%

ethanol. As a result, the saikosaponins were not efficiently separated and the purity was only around 11%. Therefore, the step-gradient elution program (1) is needed to modify to enhance the purity. From the results above, it is known that the polarity of part of impurities and saikosaponins are alike, both are relatively non-polar. However the extent of similarity in polarity between them is not known. Thus, an eluent composition 50% ethanol is added before the eluent composition of 60% ethanol in the new step-gradient elution program as shown in Fig.5.7. Since the polarity of 50% and 60% ethanol are slightly different, the former is relatively more polar, so 50% ethanol is introduced to investigate whether the impurities and the saikosaponins can be separated as a result of matching in polarity with the elution solvent.

Referring to Table 5.6 and 5.7, it is observed that nearly 900 mg impurities were eluted together with saikosaponins by 60% ethanol in the step-gradient elution program (1). On the other hand, the mass of impurities eluted together with saikosaponins by 60% ethanol in the step-gradient elution program (2) was only around 300mg. The results exhibited that the amount of impurities eluted together with saikosaponins were greatly reduced by approximately 70% if the step-gradient elution program (2) was employed. Around 70% of the total impurities originally presented in 60% ethanol eluent are now eluted by 50% ethanol eluent. It showed that

the 70% impurities were relatively more polar than the saikosaponins. It seems that the saikosaponins were efficiently separated with the impurities as the purity was greatly increased from around 11% to around 21%. However, it is also observed that a significant amount of saikosaponins was eluted by 50% ethanol eluent. As a result, the amount of saikosaponins eluted by 60% ethanol eluent was greatly minimized by over 30%. The recovery yield of the fractions collected at 60% ethanol eluent by elution program (2) was greatly decreased from about 80% to about 55%. It indicated that employing step-gradient elution program (2) could enhance the purity but reduce the recovery yield. Thus, the program (2) is needed for further modification in order to enhance the purity and recovery yield.

As the previous results shown, 50% ethanol is able to elute an amount of saikosaponins while 30% ethanol is not. Thus an eluent with an intermediate polarity was introduced to minimize the amount of saikosaponins eluted earlier and to maintain the amount of impurities eluted.

In the step-gradient elution program (3), the eluent of 50% ethanol was modified to 40% ethanol. In Fig.5.8 and Table 5.8, it can be seen that the amount of saikosaponins eluted by 40% ethanol was much less than that eluted by 50% ethanol. However, the

amount of impurities eluted by 40% ethanol was not as much as that eluted by 50% ethanol. As a result, the purity was decreased from around 21% to around 15% but the recovery yield was increased by about 10%.

Based on the results above, it is known that 40% ethanol only eluted a little amount of saikosaponins. In addition, parts of impurities could be eluted by 50% ethanol but not by 40% ethanol. Thus, 40% ethanol was modified to 45% ethanol to investigate whether 45% ethanol could elute at least the same amount of saikosaponins and greater amount of impurities than 40% ethanol. Referring to Table 5.9, greater amount of impurities as well as greater amount of saikosaponins was eluted by 45% ethanol. Even though certain amount of saikosaponins was lost in 45% ethanol eluent, the results showed that majority of saikosaponins were efficiently separated with the impurities as the purity of the fractions collected at 65% ethanol was around 20%, while the recovery yield was around 70%.

Table 5.10 The column performance indices for the 4 step-gradient elution programs

Step-gradient elution program	Purity (%)	Concentration ratio	Recovery yield (%)
(1) ^a	11.40	9:1	83.82
(2) ^a	20.89	17:1	55.31
(3) ^a	15.24	12:1	66.02
(4) ^b	20.21	17:1	68.77

a = effluent collected at 60% ethanol

b = effluent collected at 65% ethanol

Referring to Table 5.10, the purity and the concentration ratio were in the order: step-gradient elution program (4) and (2) > (3) > (1) and the recovery yield were in the order: program (1) > (4) > (3) > (2). Among the four programs, program (4) was the most proper step-gradient elution program for achieving an efficient separation as a result of high purity, high concentration ratio and acceptable recovery yield.

Referring to Table 5.9, around 70% of the total saikosaponins can be recovered in the effluent collected at 160 ml 65% ethanol. It indicated that the ratio in reduction of the bulk solution (de-bulk ratio) is around 3 times (415:160 ~ 1:2.6).

It can be seen from Table 5.6-5.9 that, the loss of saikosaponins in the adsorption step was less than 10% when the selected volume of feed solution was loaded. In addition,

around 70-80% of the total mass of concentrates was removed in the adsorption step.

It indicated that the active components were first separated in adsorption step and then further separated efficiently from the other impurities in the elution step by the proper step-gradient elution program. It showed that a completed separation process is the combination of adsorption and desorption steps.

5.2.2.4 Reusability of the column

The adsorption/desorption (A/D) cycle was repeated six times to investigate the reusability of the column and its practical applicability. The variation of breakthrough time, breakthrough capacity (adsorption capacity at breakthrough point) and the recovery yield (effluent fractions collected at 65% ethanol) with number of operation cycles were evaluated. The eluted bed was washed thoroughly with de-ionized water before being used for the next adsorption run. Table 5.11 shows the effects of A/D cycles on separation performance of column for saikosaponins.

Table 5.11 The effects of A/D cycles on separation performance of column for saikosaponins

	Breakthrough time (min)	Breakthrough capacity (BC) (mg)	Relative reduction in BC (%)	Recovery yield (%)
Cycle 1	210	136.08	100	72.38
Cycle 2	201	130.25	95.71	70.56
Cycle 3	183	118.58	87.14	68.52
Cycle 4	155	100.44	73.81	65.78
Cycle 5	111.5	72.25	53.09	62.43
Cycle 6	67	43.42	31.91	58.41

As shown in Table 5.11, the breakthrough capacity decreased when the number of cycle increased. The decrease in breakthrough capacity after repeated use of the column was attributed to the incomplete removal of impurities in the elution step. Parts of the impurities from the previous adsorption run may be trapped in the internal surface of the resin, occupied some active sites and competed with saikosaponins molecules for adsorption. As a result, less amount of saikosaponins were adsorbed in the next run. Although the capacity decreased with the cycle number, the resin retained over 50% of its original adsorption capacity after five A/D cycles. In addition, the recovery yield was decreased by less than 10%. It indicated that the effect of repeated use of the column on its elution performance was negligible. The results

showed that the column could be carried out A/D cycle for at least five times before taking regeneration. Since the resin could be reused, less amount of disposable solid wastes are generated. This corresponds to decrease in pollution and reduce the capital costs.

6. Conclusions

In the static study, the results showed that HPD100 resin had the highest equilibrium adsorption capacity on saikosaponins a, c and d. The findings indicated that the hydrophobic property of the resin play a significant role on the adsorption. The effect of surface area of the resin on the adsorption is negligible but that of average pore diameter depends on the molecular size of the analyte. A higher temperature and initial saikosaponins concentration could enhance the adsorption, but the effect of pH on adsorption is not significant. The adsorption data of saikosaponins on the HPD100 resin fitted well to the Langmuir model while those on the HPD450 and HPD600 resins fitted to either the Langmuir model or the Freundlich model. The positive value of the adsorption enthalpy and the negative value of the Gibbs free energy show that the adsorption process was endothermic and spontaneous in nature, respectively. Furthermore, the adsorption on HPD100, HPD450 and HPD600 resins followed either the pseudo first order kinetic or the pseudo second order kinetic. The rate of adsorption process was found to be controlled by the film diffusion.

In the dynamic study, the effects of the operating parameters, including feed flow rate, feed concentration and bed depth on the adsorption performance of the column were investigated. The results show the breakthrough occurred earlier when the feed flow

rate and feed concentration increased. In contrast, the breakthrough took place later when the bed depth increased. Based on the results of adsorption performance, an efficient column operation of the adsorption step in terms of loading volume and the operating time was found out. For HDP100 resin, the feed flow rate of 2 ml/min was selected and the loading volume was around 400 to 450 ml at the feed concentration of 0.300 to 0.340 mg/ml.

In the elution step, four step-gradient elution programs were evaluated and their elution performance in terms of purity, concentration ratio and recovery yield were compared. It was found that the step-gradient elution program with 120 ml 0%, 160 ml 25%, 160 ml 45%, 160 ml 65% and 120 ml 85% aqueous ethanol in succession was the most proper program to achieve an efficient separation, in which the purity, concentration ratio and recovery yield of saikosaponins were ~ 20%, ~17 and ~70% respectively. In the study of the reusability of the column, the A/D cycles were repeated six times. The results show that the column could be carried out A/D cycle for at least five times before taking regeneration.

In comparing the purity of saikosaponins in the effluent (~20.2%) with that in the crude extract (~1.2 %), it was found that the purity is greatly increased by 17 times

after a single A/D cycle. In addition, the de-bulk ratio is around 3 times. Thus, it can be concluded that separation and purification of saikosaponins by macroporous adsorption column is plausible, efficient, simple and economical.

7. Recommendations

The use of macroporous adsorption resin in separation and purification can be used as a pre-treatment step before further purification by advanced instruments e.g. preparative HPLC. Based on the results obtained, the purity of active components is enhanced by 17 times and the de-bulk ratio is around 3 times after one A/D cycle. It showed that the loading amount of the pre-treated sample for further purification is greatly minimized. Therefore, it could reduce the operating cost and increase the efficiency.

The column adsorption process can be operated in a multiple-stage process to further enhance the purity of the active components. Figure 1 shows the multiple-stage adsorption process.

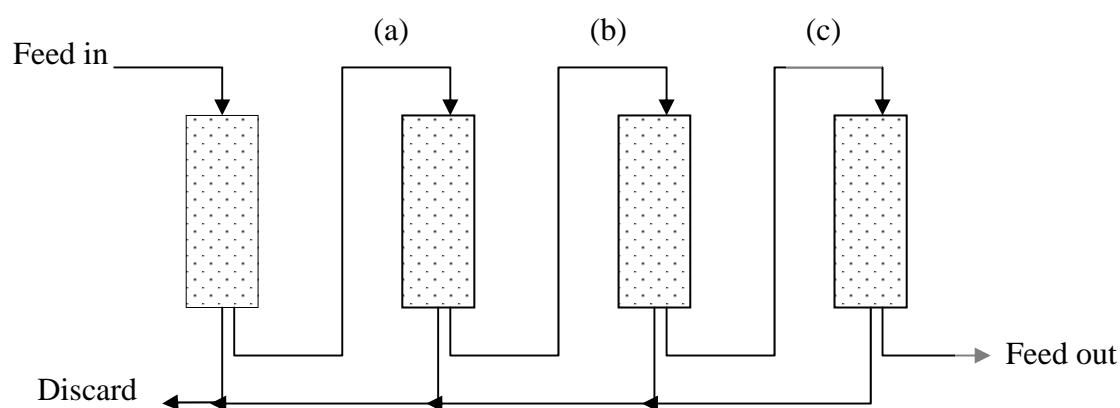


Figure 1 Flow diagram for multiple-stage adsorption process. (a), (b) and (c) are the effluents collected at 65% ethanol.

The effluent collected at 65% ethanol was re-loaded in the second column for further purification. The steps were repeated until the desirable purity of the active components was obtained.

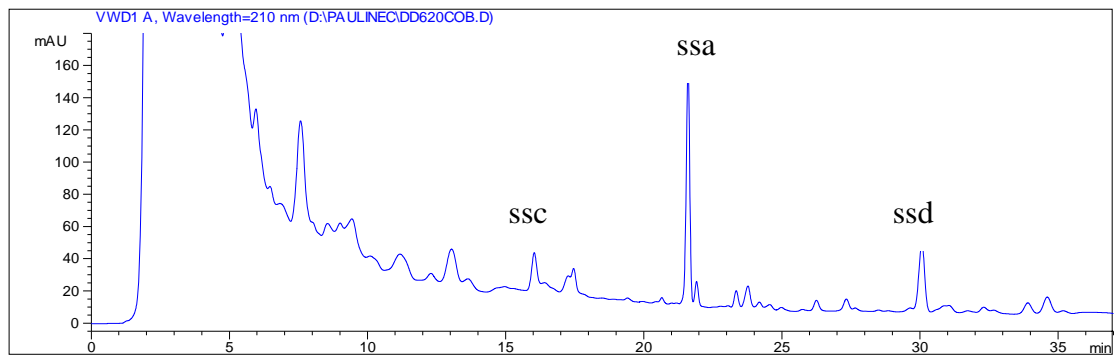
Since the detailed structures and the arrangements of functional groups of the resins are not known, it is necessary to conduct experiments to get more information of the structure of the resins, thus, the microscopic interactions between the resins and the saikosaponins molecules will be clearer.

8. Appendices

Appendix A.1

HPLC chromatogram of the saikosaponins a, c and d in the crude Chai Hu extract

A.1-1 HPLC chromatogram of the saikosaponins a, c and d in the crude Chai Hu extract



Appendix A.2

Data analysis – ANOVA: Two Factors Without Replication

A.2-1 The r^2 of two isotherm models for HPD100

Temperature (K)	Langmuir model r^2	Freundlich model r^2
288	0.996	0.953
298	0.991	0.934
308	0.997	0.957

A.2-2 Results of ANOVA analysis for HPD100 (at $\alpha = 0.05$)

Source of Variation	SS	df	MS	F	P-value	F crit
Rows	0.00024	2	0.00012	2.919028	0.255165	19.00003
Columns	0.003267	1	0.003267	79.35223	0.012369	18.51276
Error	8.23E-05	2	4.12E-05			
Total	0.003589	5				

Referring to A.2-2, since $F > F$ crit, there is a significant difference between the r^2 of the two isotherm models.

A.2-3 The r^2 of two isotherm models for HPD450

Temperature (K)	Langmuir model r^2	Freundlich model r^2
288	0.982	0.943
298	0.944	0.989
308	0.981	0.985

A.2-4 Results of ANOVA analysis for HPD450 (at $\alpha = 0.05$)

Source of Variation	SS	df	MS	F	P-value	F crit
Rows	0.000472	2	0.000236	0.267712	0.788823	19.00003
Columns	1.67E-05	1	1.67E-05	0.018893	0.903263	18.51276
Error	0.001764	2	0.000882			
Total	0.002253	5				

Referring to A.2-4, since $F < F$ crit, there is no significant difference between the r^2 of

the two isotherm models.

A.2-5 The r^2 of two isotherm models for HPD600

Temperature (K)	Langmuir model r^2	Freundlich model r^2
288	0.934	0.962
298	0.865	0.937
308	0.895	0.961

A.2-6 Results of ANOVA analysis for HPD600 (at $\alpha = 0.05$)

Source of Variation	SS	df	MS	F	P-value	F crit
Rows	0.002225	2	0.001113	3.908665	0.203721	19.00003
Columns	0.004593	1	0.004593	16.13349	0.056757	18.51276
Error	0.000569	2	0.000285			
Total	0.007387	5				

Referring to A.2-6, since $F < F$ crit, there is no significant difference between the r^2 of the two isotherm models.

A.2-7 The r^2 of two kinetic models for HPD100, HDP450 and HPD600

Resins	Pseudo first-order model r^2	Pseudo second-order model r^2
HPD100	1	0.995
HPD450	0.999	0.991
HPD600	0.989	0.999

A.2-8 Results of ANOVA analysis for the three resins (at $\alpha = 0.05$)

Source of Variation	SS	df	MS	F	P-value	F crit
Rows	1.3E-05	2	6.5E-06	0.139785	0.877358	19.00003
Columns	1.5E-06	1	1.5E-06	0.032258	0.874012	18.51276
Error	9.3E-05	2	4.65E-05			
Total	0.000108	5				

Referring to A.2-8, since $F < F$ crit, there is no significant difference between the r^2 of the two kinetic models.

References

- Chen, K. and Chen, T (2004). Wind-Heat Releasing Herbs. Art of Medicine Press, Inc., chapter 1, section 2.
- Dong, A.W., Tang, C.Y., Xiang, Z., Peng, J.H., Lin, G.Y. and He, Z (2004). Research on Adsorption Separation of Red Pigment in *Parthenocissus Tricuspidate Planch* by HPD-600 Resin and Characteristics of Red Pigment. Food Science, 25(4), 74-80.
- Dong, F. Y (2001).現代實用中藥新劑型新技術。人民衛生出版社。
- Dong, W.B., Hu, Y. and Zhang, J.H (2002). Study on Macroporous Resin Adsorbing Technology for preparing the high purity TP product. Journal of Northwest University of Light Industry, 20, 1-8.
- Feng, J. G. and Gu, W. Y (2003). The Adsorption and Desorption Properties of Macroporous Resins for Soybean Isoflavone. Journal of Wuxi University of Light Industry, 22(1), 82-85.
- Frank L. Slejko (1985). Adsorption Technology: A Step-by-Step Approach to Process Evaluation and Application. Marcel Dekker, Inc.
- Fung, X. Z., Chen, Y. C. and Yang, J. S (1979). The study of chemical components in *Gastrodia Elata*. Acta Chimica Sinica, 37(3):175.
- Gao, H.N., Jn, W.Q., Guo, L.W., Zhuang, H. and Zhang, Z.L (2001). Adsorption properties of AB-8 resin for purification of total flavone in *Sophora flavescens*. Chinese Traditional and Herbal Drugs, 32(10), 887-889.
- Heidelbert, W., Rudolf, B., Xiao, P.G., Chen, J.M. and Franziska, O (1996). Chinese Drug Monographs and Analysis, Radix Bupleuri (Chai Hu) 1(1).
- Jin, J. L., Ren, D.X., Jin, Z.Z., Cui, H., Han, L.Z., Piao, H.S. and Li, Y.J (1999). Extraction of *Tribulus terrestris* L. saponins by macroreticular resin. Journal of Medical Science Yanbian University, 22(1), 29-31.
- Jung, Y. L., Surk, S. M. and Byung, K. H (2003). Isolation and Antifungal and Antioomycete Activities of Aerugine Produced by *Pseudomonas fluorescens* Strain

MM-B16. Applied and Environmental Microbiology, 69(4), 2023-2031.

Kalavathy, M.H., Karthikeyan, T., Rajgopal, S. and Miranda, L.R (2005). Kinetic and isotherm studies of C(II) adsorption onto H₃PO₄ – activated rubber and sawdust. Journal of Colloid and Interface Science, 292, 354-362.

Klaus, S. and Hans, J.F (1995). Thermal Separation Process – Principles and Design. Weinheim (New York), Chapter 4.

Kyriakopoulos, G., Doulin, D. and Anagnostopoulos, E (2005). Adsorption of pesticides on porous polymeric adsorbents. Chemical Engineering Science, 60, 1177-1186.

Li, C.X., Yin, S.G., Wang, K.L. and He B.L (1994). Study on the Adsorption of Gypenosides by Macroporous Adsorbent Resins. Ion exchange and adsorption, 10(3), 203-207.

Li, F.M., Sun, S.Y., Wang, J. and Wang, D.W (1998). Chromatography of Medicinal Plants and Chinese Traditional Medicines. Biomedical Chromatography, 12, 78-85.

Li, H.B. and Li, X.M (2005). Application of Macroporous Adsorbing Resins in Natural Products Research. Guangdong Chemical Industry, 3, 22-25.

Liu, Z.Q., Cai, X., Lai, X. P., Zhu, C.C. and Liu, L (2001). Studies on Purification of Panax Notoginseng Saponins (PNS) with Macroporous Resin. Chinese Journal of Experimental Traditional Medical Formulae, 7(3), 4-6.

Lu, M.C., Di, Z., Xie, M.J., Liu, Y.X., Yu, H.S. and Jin, F.X (2004). Properties of Macro-pore Resin Absorbing Soybean Isoflavone. Food and Fermentation Industries, 30(1), 92-95.

Ma, X.P., Jiang, C.H., Yang, Y.Q. and Zhang, L. Y (1997). A Study on the Adsorption of flavonoids in Ginkgo biloba L. Leaves by Macroporous Adsorptive Resins. China journal of Chinese materia medica, 22(9), 539-542.

Meng, Q. and Zhang, B (1999). Research on The Characteristics of Shikonin Adsorption and Separation of Shikonin from cell culture medium using Macroporous Resin. Ion exchange and adsorption, 15(1), 36-42.

Mi, J.Y. and Song, C.Q (2001). Advances of Application of Macroporous Resin in Study of Traditional Chinese Herbs. *Chinese Traditional Patent Medicine*, 23 (12), 914-917.

Pan, J., Chen, Q., Xie, H.M., Zhang, J. and Wang, G.X (1999). Performance of Adsorption and Separation of the Macroporous Resin for Pueraria Iosflavones. *Transactions of the CSAE*, 15(1), 236-240.

Peter Atkins (2001). *The Element of Physical Chemistry (Third Edition)*. Oxford University Press, Chapter 4 and 7.

Qi, B. and Gu, W.Y (2005). Study on adsorption and separation of macroporous resin for flavonoids from *P. sibiricum* Redoute. *Food & Machinery*, 21(2), 14-16.

Shanghai Institute of Materia Medica, Chinese Academy of Sciences (1983). *Extraction and isolation of active components in Chinese Herbs (Second Edition)*. Shanghai Scientific and Technical Publishers.

The State Pharmacopoeia Commission of P.R. China (2000). *Pharmacopoeia of the People's Republic of China (English Edition)*. Chemical Industry Press, volume 1.

Thurman, E.M. and Mills, M.S (1998). *Solid-Phase Extraction: Principles and Practice*. John Wiley & Sons, Inc., Chapter 2.

Tu, P. F., Jia, C.Q. and Zhang, H.Q (2004). Application of Macroporous Adsorption Resins to Study and Production of TCM New Drugs. *World Science and Technology*, 6(3), 22-28.

Wang, J.F., Xue, D. and Cang, J (2001). The Application of Separation and Purification of Effective Elements in Chinese Herbal Medicine by Macroporous Adsorptive Resin. *Hunan Guiding Journal of TCMP*, 7(3), 125-126.

Wang, Z., Ping, Q.N. and Huang, L. S (2004). Study on adsorption of crocin in gardenia with macroporous resin. *Chinese Traditional Patent Medicine*, 26(7), 532-534.

Warren, L. M., Julian C.S. and Peter, H (2005). *Unit Operations of Chemical Engineering*, 7th Edition, Chapter 25.

Wei, R.X., Chen, J.L., Chen, L.L., Fei, Z. H., Li, A.M. and Zhang, Q.X (2004). Study of adsorption of lipoic acid on three types of resin. *Reactive and Functional Polymers*, 59, 243-252.

World Health Organization (WHO) monographs on selected medicinal plants (1999). Genera 1, 67-76.

Wu, H., Liang, H., Wu, D.C. and Yuan, Z. H (2003). Isolation and purification of total saponins from *Cornus Officinalis* by column chromatography of macroreticular resin. *J. Fourth. Mil. Med Univ.*, 24(8), 689-692.

Xiao, W.X., Zhong, J., Wang, X.G. and Xiao, H (2000). Separation and preparation of tea polyphenols by adsorption resin chromatography. *Natural Product Research and Development*, 11(6), 44-49.

Xu, Z.Y., Zhang, Q.X. and Fang, H.P (2002). Applications of Porous Resin Sorbents in Industrial Wastewater Treatment and Resource Recovery. <http://www.paper.edu.cn>.

Yi, W., Yang, M., Quan, B. Z. and Han, Q.Y (2005). Isotherms, kinetics and thermodynamics of dye biosorption by anaerobic sludge. *Separation and Purification Technology*.

Zeng, (1992).The effect of inorganic salts on the adsorption of ginsenosides by Macroporous adsorption resin. *Chinese Journal of Pharmaceuticals*, 23(8), 339-342.

Zhang, H., Tong, M. R., Pan, J.L. and Yu, Y. T (1995). Separation of Camptothecin by Macroporous Resin Adsorption. *Ion exchange and adsorption*, 11(2), 145-150.

Zhang, Q. and Chen, Y (1999). The Adsorbing Ability of AB-8 Macro-porous Resin for Perilla Pigment – Determination of the Adsorption Isotherm and Flowing Adsorption Curve at pH =3. *Food and Fermentation Industries*, 25(3), 16-19.

Zhang, W.M., Chen, J.L., Pan, B.C., Zhang, Q. and Xing, B.Z (2006). *Journal of Hazardous Materials*.

Zhang, X.L., Xue, W. M., Li, P. and Kang, M.D (2001). Adsorptive Separation based on Resins for Tea-Polyphenols and Caffeine. *Chemical Engineering (China)*, 29(3), 15-19.

Zheng, H., Yu, Y. Z., Wu, W.T., Zhong, Y. and Han Z.Q (2003). Studies on isolation and purification of abscisic acid by macroreticular resin adsorbent method. *Chinese Journal of Antibiotics*, 28(11), 653-655.

Zheng, Y.L., Zhang, C.X., Zhang, C. H., Fu, R.L., Geng, Y. Q and Ren, H.J (2002). Effect of D-101 Macro Reticular Resin on Adsorptive Capacity of Ginsenoside. *Journal of Jilin Agricultural University*, 24(6), 47-49.

Zhong, L. M., Xia, X. H. and Li, B (2004). Static adsorption and desorption capabilities of five different macroporous resin for purifying total saponins of *Polygala Fallax Hemsl.* *Chinese Traditional Patent Medicine*, 26(6), 446-448.